Non-equilibrium statistical mechanics of the stochastic Navier–Stokes equations and geostrophic turbulence

Freddy Bouchet, Cesare Nardini and Tomás Tangarife

Abstract Two-dimensional and geophysical turbulent flows have the property to self organize and create large scale coherent jets and vortices. This is for instance one of the major processes for the dynamics of Earth's atmosphere. Following Onsager initial insight, based on conjugated works by mathematicians and physicists, this fundamental physical process has found some explanations in the framework of statistical mechanics. An important step, initiated twenty years ago, has been the study of the equilibrium statistical mechanics for the 2D Euler and the related quasi-geostrophic models (the Miller-Robert-Sommeria theory).
Real geophysical and experimental flows are however dissipative and maintained by external forces. These lectures focus on recent theoretical development of the statistical mechanics of those non-equilibrium situations. Those progresses have been achieved using tools from field theory (path integrals and instantons), non-equilibrium statistical mechanics (large deviations, stochastic averaging). The aim of these lectures is to briefly introduce the theoretical aspects of this program in the simplest context: the 2D stochastic Euler or Navier-Stokes equations and the quasi-geostrophic equations.
We review path integral representations of stochastic processes, large deviations for transition probabilities, action minimization, instanton theory, for general mechanical systems forced by random forces. We will apply this framework in order to predict equilibrium and non-equilibrium phase transitions for the 2D Euler, Navier-Stokes, and quasi-geostrophic dynamics, and to predict the rates of rare transitions between two attractors in situations of first order phase transitions.
Kinetic theory of systems with long range interactions, both with and without stochastic external forces, are explained. Based on this kinetic theory, we predict non-equilibrium phase transitions, and discuss their recent experimental observations and numerical simulations.
Even if the model we have considered so far are too simple academic models, the ex-

Freddy Bouchet, Laboratoire de physique, École Normale Supŕieure de Lyon et CNRS, 46 allée d'Italie, 69007 Lyon, France. E-Mail: Freddy.Bouchet@ens-lyon.fr.

pected relevance of those approaches in the future for Earth atmosphere and climate dynamics is briefly discussed.

1 Introduction

1.1 Self-organization of two-dimensional and geophysical flows

Atmospheric and oceanic flows are three-dimensional (3D), but are strongly dominated by the Coriolis force mainly balanced by pressure gradients (geostrophic balance). The turbulence that develops in such flows is called geostrophic turbulence. Models describing geostrophic turbulence have the same type of additional invariants as those of the two-dimensional (2D) Euler equations. As a consequence, energy flows backward and the main phenomenon is the formation of large scale coherent structures (jets, cyclones and anticyclones). One such example is the formation of Jupiter's Great Red Spot, Fig. 1.

Fig. 1 Picture of Jupiter's Great Red Spot - a large scale vortex situated between bands of atmospheric jets. Photo courtesy of NASA: http://photojournal.jpl.nasa.gov/catalog/PIA00014.

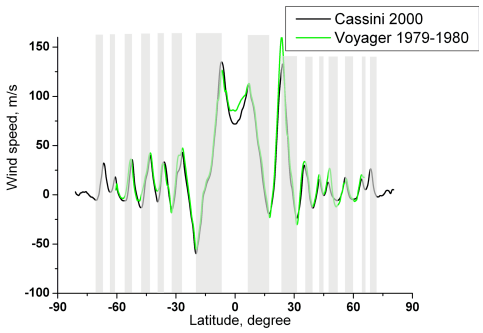

Fig. 2 Zonally averaged velocity profile in the upper troposphere of Jupiter. The flow is organised into alternating strong jets.

The analogy between 2D turbulence and geophysical turbulence is further emphasized by the theoretical similarity between the 2D Euler equations, describing 2D flows, and the layered quasi-geostrophic or shallow water models, describing the largest scales of geostrophic turbulence: both are transport equations for a scalar quantity by a non-divergent flow, conserving an infinite number of invariants.

The formation of large scale coherent structures is a fascinating problem and an essential part of the dynamics of Earth's atmosphere and oceans. This is the main motivation for setting up a theory for the self-organization of 2D turbulence.

1.2 Statistical mechanics of the self-organization of two-dimensional and geophysical flows: Onsager's equilibrium route

Any turbulence problem involves a huge number of degrees of freedom coupled via complex nonlinear interactions. The aim of any theory of turbulence is to understand the statistical properties of the velocity field. It is thus extremely tempting to attack these problems from a statistical mechanics point of view.

Statistical mechanics is indeed a very powerful set of theoretical tools that allows us to reduce the complexity of a system down to a few thermodynamic parameters. As an example, the concept of phase transition allows us to describe drastic changes of the whole system when a few external parameters are changed. Statistical mechanics is the main theoretical approach we develop in these lectures. It succeeds in explaining many of the phenomena associated with two-dimensional turbulence [13].

This may seem surprising at first, as it is a common belief that statistical mechanics is not successful in handling turbulence problems. The reason for this belief is that most turbulence problems are intrinsically far from equilibrium. For instance, the forward energy cascade in three-dimensional turbulence involves a finite energy dissipation, no matter how small the viscosity (anomalous dissipation) (see for instance Onsager's insightful consideration of the non-conservation of energy by the three dimensional Euler equations [28]). As a result of this finite energy flux, three dimensional turbulent flows cannot be considered close to some equilibrium distribution.

By contrast, two-dimensional turbulence does not suffer from the anomalous dissipation of the energy, so equilibrium statistical mechanics, or close to equilibrium statistical mechanics makes sense when small fluxes are present. The first attempt to use equilibrium statistical mechanics ideas to explain the self-organization of two-dimensional turbulence dates from Onsager work in 1949 [51] (see [28] for a review of Onsager's contributions to turbulence theory). Onsager worked with the point-vortex model, a model that describes the dynamics of singular point vortices, first used by Lord Kelvin and which corresponds to a special class of solutions of the 2D Euler equations. The equilibrium statistical mechanics of the point-vortex model has a long and very interesting history, with wonderful pieces of mathematical achievements [51, 37, 18, 39, 26, 21, 27, 1].

The generalization of Onsager's ideas to the 2D Euler equations with a continuous vorticity field, taking into account all invariants, has been proposed in the beginning of the 1990s [57, 45, 58, 60], leading to the Miller–Robert–Sommeria

theory (MRS theory). The MRS theory includes the previous Onsager theory and determines within which limits the theory will give relevant predictions and results.

The MRS theory deals with the microcanonical invariant measure. It predicts that most microscopic states (vorticity field) concentrate into a single macrostate (most vorticity fields basically have the same large scale velocity field). This explains why one should expect the flow to self-organize into this equilibrium macrostate. This equilibrium macrostate is characterized by the maximization of an entropy with some constraints related to dynamics invariants. The aim of section 3 is to sketch the derivation of this variational problem, which is the basis of the theory. Then application to the Great Red Spot of Jupiter will be briefly summarized.

These two points constitute a very brief overview of equilibrium statistical mechanics. Over the last fifteen years, the RSM equilibrium theory has been applied successfully to a large class of problems, for both the two-dimensional Euler and quasi-geostrophic equations. This includes many interesting applications, such as the predictions of phase transitions in different contexts, a model for the Great Red Spot and other Jovian vortices, and models of ocean vortices and jets. A detailed description of the statistical mechanics of 2D and geophysical flows (theory) and of these geophysical applications is presented in the review [13]. Older reviews or books [64, 42, 40], give a very interesting complementary viewpoint, stressing mainly the theory and laboratory experiments. The note by Y. Pomeau [54] gives also a very interesting comment on the reason why the two-dimensional Euler equations, by contrast with most other equilibrium approach for classical field theory, does not suffer from the Rayleigh-Jeans paradox (basically the fact that a classical field has an infinite heat capacity). This point is further discussed in [13]. Finally we stress that equilibrium statistical mechanics for two dimensional and geophysical flows is still a very active subject, with many contribution during the last few years [71, 70, 33, 34, 35, 66, 49, 48, 73, 8, 24, 55], many of them by bright young scientists.

As far as equilibrium statistical mechanics is concerned, the aim of these lecture is just to explain the basis of Miller–Robert–Sommeria theory, explain how to compute the entropy of macrostate and thus their probability through the use of large deviation theory. We discuss these points in section 3 at a level which is as elementary as possible.

1.3 Non-equilibrium statistical mechanics of the self-organization of two-dimensional and geophysical flows: statistical mechanics and dynamics

Most of natural turbulent flows are not freely evolving, they are rather constantly forced and dissipated. Then, in statistically stationary regimes, power input through external forces balance energy dissipation on average. In the limit of very small forces and dissipation, compared to conservative terms of the dynamics, it is ex-

pected to find a strong relation between these non-equilibrium flows and some of the states predicted by equilibrium statistical mechanics. In order to give a precise meaning to this general idea, and to deal with far from equilibrium situations, it is essential to develop also the non-equilibrium statistical mechanics of the 2D Euler, 2D Navier-Stokes and barotropic quasi-geostrophic equations. As we discuss below, this has been the subject of recent key advances in the applications of statistical mechanics to turbulent flows. This is actually the main subject of these lectures.

We present two non-equilibrium statistical mechanics approaches: the first deals with non-equilibrium first order phase transitions and the computation of transition rates using large deviations, and the second is a kinetic theory approach to the prediction of the large scale flows.

1.3.1 Statistical mechanics of paths in phase space and non-equilibrium bistable turbulent flows

Many turbulent flows can evolve and self-organize towards two or more very different states. In some of these systems, the transitions between two of such states are rare and occur relatively rapidly. Examples include the Earth magnetic field reversals (over geological timescales) or in magnetic field reversal in MHD experiments (e.g. the Von Krmn Sodium (VKS) turbulent dynamo in Fig. 3) [3], Rayleigh-Bnard convection cells [20, 50, 65, 17], 2D turbulence [63, 41, 10] (see Fig. 4), 3D flows [56] and for ocean and atmospheric flows [72, 62]. The understanding of these transitions is an extremely difficult problem due to the large number of degrees of freedoms, large separation of timescales and the non-equilibrium nature of these flows.

However, for forced-dissipated turbulent systems it is unclear how to define the set of attractors for the dynamics. Although, in the limit of weak forcing and dissipation, one would expect that the set of attractors would converge to the ones of the deterministic equation. In the case of the 2D Euler equations, equilibrium statistical mechanics in the form of the equilibrium Miller-Robert–Sommeria theory allows for the prediction set of attractors for the dynamics. They are a subsets of the steady states of the 2D Euler equations, then equilibrium statistical mechanics gives a first partial answer to the question of attractors.

Moreover, simulations of the 2D Navier-Stokes equations in the weak force and dissipation limit showed that the dynamics actually concentrates precisely close to the set of the 2D Euler equations attractors [10]. Interestingly, the same simulation showed sporadic non-equilibrium phase transitions, where the system spontaneously switched between two apparently stable steady states resulting in a complete change in the macroscopic behavior (see figure 4). If the forces and dissipation are weak, then these transitions are actually extremely rare, occurring on a timescale much longer than the dynamical timescale.

In such situations, when the turbulent flow switches at random times from one type of attractor to another, a theoretical aim is to compute the transition rate. It is also often the case that most transition paths from one attractor to another concentrate to a single path, then a natural aim is to compute this most probable path.

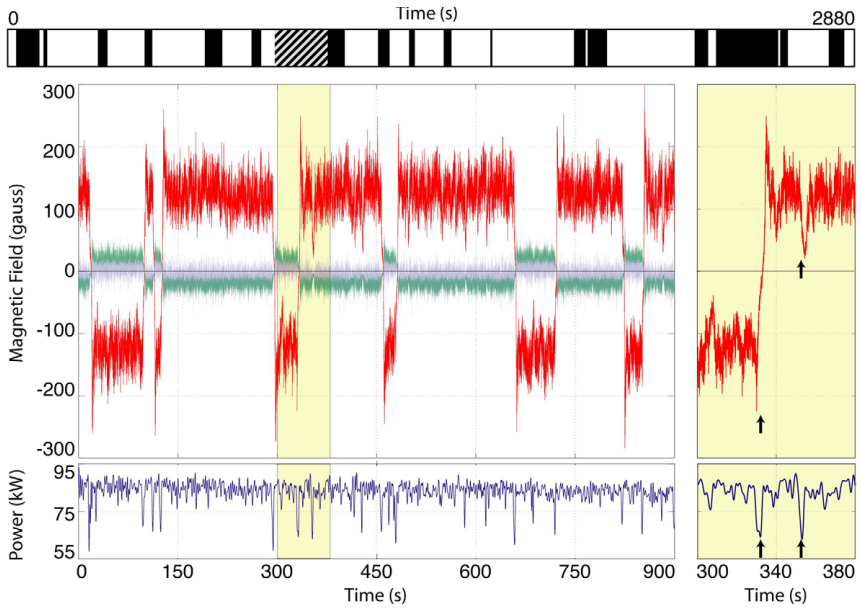

Fig. 3 Figure taken from [3] showing random transitions between meta-stable orientations of the magnetic field in an experimental turbulent dynamo. The main azimuthal component of the magnetic field is shown in red.

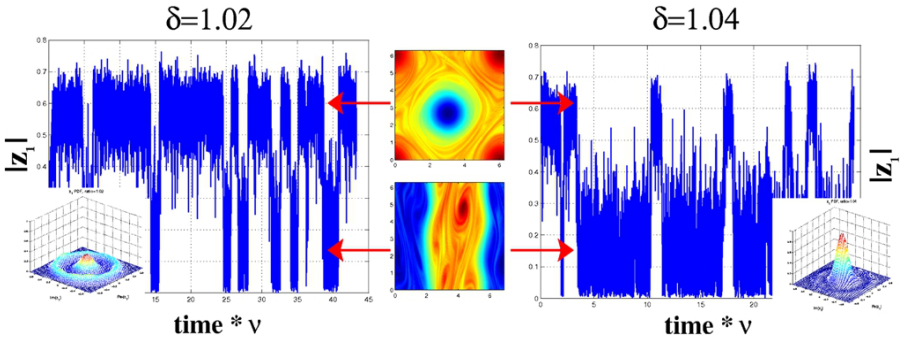

Fig. 4 Figure taken from [10] showing rare transitions (illustrated by the Fourier component of the largest y mode) between two large scale attractors of the periodic 2D Navier-Stokes equations. The system spends the majority of its time close to the vortex dipole and parallel flows configurations.

In order achieve those aims, we will use a path integral representation of the transition probabilities and study its semi-classical limit, in an asymptotic expansion where the small parameter is the one that determines both the force and dissipation amplitude. In this limit, if this semi-classical approach is relevant, one expects a large deviation result, similar to the one obtained through the Freidlin-Wentzell theory[30]. In order to illustrate in a pedagogical way the general approach, we will treat in these lectures the classical case of the Kramer model (computation of the

transition rate for a particle in a double well potential). We will generalize the discussion to a set of Langevin dynamics that includes the two-dimensional Euler and Quasi-Geostrophic Langevin dynamics, and finally we will discuss partial results for the two-dimensional Navier-Stokes equations when detailed balance is not satisfied. Those different points are discussed in section 4.4.

1.3.2 Kinetic theory of zonal jets

One example of spontaneous emergence of large-scale coherent structures in geophysical flows is the formation of zonal (east-west) jets. The common pictures of Jupiter perfectly illustrate this fact: the surface flow is clearly organized into parallel, alternating zonal jets as shown in figure 2, with also the presence of giant and very stable vortices such as the Great Red Spot. Such large scale features are on one hand slowly dissipated, mainly due to a large-scale friction mechanism, and on the other hand maintained by the small-scale turbulence, through Reynolds' stresses. The main mechanism is thus a transfer of energy from the forcing scale (due to barotropic and baroclinic instabilities) to the turbulent scales and until the scale of the jets.

An important point in this phenomenology is the fact that the turbulent fluctuations are of very weak amplitude compared to the amplitude of the zonal jet, and that they evolve much faster. This means that the typical time scale of advection and shear of the fluctuations by the jet is much smaller that the typical time scale of formation or dissipation of the whole jet. This time scale separation is a very specific property of the geophysical large-scale structures.

In this turbulent context, the understanding of jet formation requires averaging out the effect of rapid turbulent degrees of freedom in order to describe the slow evolution of the jet structure. Such a task, an example of closure, is usually extremely hard to perform for turbulent flows. Using the time-scale separation mentioned earlier, we prove that it can be performed explicitly in this problem. This approach, called a kinetic theory by analogy with similar approaches in the statistical mechanics of systems with long range interactions, is presented in section 5.

1.4 A contemporary approach of statistical mechanics: large deviation theory

Onsager was the first to consider a statistical mechanics explanation of two-dimensional turbulent flows [51]. At the time he was scientifically active, Onsager made a large number of decisive contributions to statistical mechanics theory: solutions of the 2D Ising model, reciprocity relations, contributions to the statistical mechanics of electrolytes and turbulence, and so on. Since that time the theoretical approaches for treating statistical mechanics problems have been completely renewed. One of the main changes has been the use of the language of large deviation theory for

more than 30 years. For instance, recent results in the understanding of equilibrium statistical mechanics problems, proving fluctuation theorems (Onsager's reciprocity relations generalized far from equilibrium), and in dealing with non-equilibrium statistical mechanics problems, are all related to large deviation theory.

Interestingly, as we discuss in these lectures, the route proposed by Onsager in his 1949 paper [51] in order to understand the self-organization of two-dimensional flows, led a few decades later to some of the first applications of large deviation theory to equilibrium statistical mechanics problems.

The theory of large deviations deals with the asymptotic behavior of the exponential decay of the probabilities of rare or extreme events. The associated limiting parameter is usually taken to be the number of observations, the number of particles, but can be other parameters, such as vanishing noise or the temperature of a chemical reaction, or large time. Large deviation theory can be considered a generalization of the central limit theorem, with the refinement of including information about the behavior of the tails of the probability density. The main result of large deviation theory is the large deviation principle, a result describing the leading asymptotic behavior of the tails or large deviations of the probability distribution in the limit $N \to \infty$. For instance, the large deviation principle for a random variable X_N is

$$\lim_{N\to\infty} -\frac{1}{N}\log[P(X_N = x)] = I(x), \tag{1}$$

where P is the probability density for the random variable X_N, and $I(x)$ is called the rate function. For instance, if $X_N = (1/N)\sum_{i=1}^{N} x_i$, where x_i are independent identically distributed random variables then $I(x)$ is given by Cramer's theorem.

Beside the applications described in the previous sections, the aim of these lectures is to explain and derive heuristically large deviation results for the equilibrium statistical mechanics of the two-dimensional Euler and quasi-geostrophic equations (equilibrium) and for the 2D Navier-Stokes or quasi-geostrophic equations with stochastic forces (non-equilibrium). The large deviation result for the equilibrium case (section 3) is derived through a generalization of Sanov theorem, and leads to a formula for the probability of macrostates for the microcanonical measures. The large deviation results for the non-equilibrium cases (section 4.4) are derived through semi-classical limits in path integrals (or equivalently the Freidlin-Wentzell framework) and lead to the evaluation of transition paths and transition probabilities for bistable turbulent flows, close to non-equilibrium phase transitions.

1.5 Organization of those lectures

In section 2, we state the equations of motion and their conservation laws. In section 3, we construct microcanonical invariant measures for the 2D Euler equations and discuss the entropy maximization problem in predicting the most probably steady states on the 2D Euler equation. In section 4.4, we discuss large deviations for non-equilibrium problems and illustrate this using a simple academic example,

the problem of computation of transition rate for the Kramer problem, followed by the application to the 2D Navier-Stokes equations. Finally, in section 5 we discuss the kinetic theory of zonal jets for the barotropic quasi-geostrophic dynamics.

2 The 2D Euler, barotropic Quasi Geostrophic, and stochastic Navier–Stokes equations

2.1 Equations of motion

The aim of this section is to present the simplest model that describes two-dimensional and geophysical turbulent flows: the two-dimensional Navier-Stokes equation and the barotropic equation with stochastic forcing. In the limit when forces and dissipation go to zero, the two-dimensional Navier-Stokes equation reduces to the two-dimensional Euler equation. We describe the conservation laws for these equations and their influence on the dynamics. The review [13] gives a very brief introduction to geophysical fluid dynamics and the quasi-geostrophic model. A more complete introduction is found in textbooks of geophysical fluid dynamics [53, 68].

We are interested in the non-equilibrium dynamics associated to the two-dimensional stochastically forced barotropic equations (also called barotropic Quasi-Geostrophic equations):

$$\frac{\partial q}{\partial t} + \mathbf{v}\,[q-h]\cdot\nabla q = -\alpha\omega + \nu\Delta\omega + \sqrt{2\alpha}\eta, \tag{2}$$

$$\mathbf{v} = \mathbf{e}_z \times \nabla\psi, \qquad q = \omega + h(y) = \Delta\psi + h, \tag{3}$$

where ω, $\mathbf{v}$ and ψ are respectively the vorticity, the non-divergent velocity, and the streamfunction. For simplicity, in these lectures we consider the dynamics on a periodic domain $\mathscr{D} = [0, 2\delta\pi) \times [0, 2\pi)$ with aspect ratio δ. Then ψ is periodic with the further condition $\int_{\mathscr{D}} \mathrm{d}\mathbf{r}\ \psi = 0$. q is the potential vorticity, and h is a given topography function with $\int_{\mathscr{D}} \mathrm{d}\mathbf{r}\ h = 0$. For $h = 0$, the barotropic equations reduces to the 2D Navier-Stokes equation.

The linear friction term $-\alpha\omega$ models large scale dissipation. We consider non-dimensional equations, where a typical energy is of order 1 (see [13]) such that ν is the inverse of the Reynolds number and α is the inverse of a Reynolds number based on the large scale friction. We assume that the Reynolds numbers satisfy $\nu \ll \alpha \ll 1$. In the limit of weak forces and dissipation $\lim_{\alpha\to 0}\lim_{\nu\to 0}$, the 2D Navier-Stokes equations converge to the two-dimensional Euler equations for finite time, but the type of forcing and dissipation determines to which set of attractors the dynamics evolve to over a very long time. The curl of the forcing $\eta(\mathbf{x},t)$ is a white in time Gaussian field defined by $\langle \eta(\mathbf{x},t)\eta(\mathbf{x}',t')\rangle = C(\mathbf{x}-\mathbf{x}')\delta(t-t')$, where C is the correlation function of a stochastically homogeneous noise.

The two-dimensional Euler equations ($h = 0$), or the inertial barotropic equation ($h \neq 0$), are given by Eq. (2) with forces and dissipation set to zero ($\alpha = \nu = 0$).

2.2 Conservation laws for the inertial dynamics

The kinetic energy of the flow is given by

$$\mathscr{E}[q] = \frac{1}{2}\int_{\mathscr{D}} \mathrm{d}\mathbf{r}\, \mathbf{v}^2 = \frac{1}{2}\int_{\mathscr{D}} \mathrm{d}\mathbf{r}\, (\nabla\psi)^2 = -\frac{1}{2}\int_{\mathscr{D}} \mathrm{d}\mathbf{r}\, (q-h)\psi, \tag{4}$$

where the last equality is obtained with an integration by parts. The kinetic energy is conserved for the dynamics of the two-dimensional Euler and inertial barotropic equations i.e. $\mathrm{d}\mathscr{E}/\mathrm{d}t = 0$,. These equations also conserve an infinite number of functionals, named Casimirs. They are related to the degenerate structure of the infinite-dimensional Hamiltonian system and can be understood as invariants arising from Noether's theorem [61]. These functionals are of the form

$$\mathscr{C}_s[q] = \int_{\mathscr{D}} s(q)\, \mathrm{d}\mathbf{r}, \tag{5}$$

where s is any sufficiently regular function. We note that on a doubly-periodic domain the total circulation

$$\Gamma = \int_{\mathscr{D}} q\, \mathrm{d}\mathbf{r}, \tag{6}$$

is necessarily equal to zero: $\Gamma = 0$.

The infinite number of conserved quantities are responsible for the equations having an infinite (continuous) set of steady states (see section 2 in [13]). Any of the infinite number of steady states of the 2D Euler or inertial barotropic equations satisfy

$$\mathbf{v}\cdot\nabla q = 0.$$

For instance, if there is a functional relation between the potential vorticity and the streamfunction, i.e. $q = \Delta\psi = f(\psi)$, where f is any continuous function, then using 2 one easily check that $\mathbf{v}\cdot\nabla q = 0$. Physically, these states are important because some of them act as attractors for the dynamics.

There is also a strong empirical and numerical evidence that a complex evolution of the two-dimensional Euler equations leads most of the times to attractors that are steady states of the equations. The specific function f that is reached after a complex evolution can be predicted in certain situation using equilibrium statistical mechanical arguments presented in the next section (see [13] for more details).

2.3 The conservation of the vorticity distribution

The two-dimensional Euler and inertial barotropic equations conserve the distribution of potential vorticity, i.e. the total area of a specific potential vorticity level set is conserved. As we explain now the conservation of the potential vorticity distribution is equivalent to the conservation of all Casimirs.

We first prove that the potential vorticity distribution is conserved as a consequence of Casimir conservation laws. We consider the special class of Casimir (5):

$$C(\sigma) = \int_{\mathscr{D}} H(-q+\sigma)\,\mathrm{d}\mathbf{r}, \tag{7}$$

where $H(\cdot)$ is the Heaviside step function. The function $C(\sigma)$ returns the area occupied by all potential vorticity levels smaller or equal to σ. $C(\sigma)$ is an invariant for any σ and therefore any derivative of $C(\sigma)$ is also conserved. Therefore, the distribution of vorticity, defined as $D(\sigma) = C'(\sigma)$, where the prime denotes a derivation with respect to σ, is also conserved by the dynamics. The expression $D(\sigma)d\sigma$ is the area occupied by the vorticity levels in the range $\sigma \leq q \leq \sigma + d\sigma$.

Moreover, any Casimir can be written in the form

$$\mathscr{C}_f[q] = \int_{\mathscr{D}} \mathrm{d}\sigma\, f(\sigma) D(\sigma).$$

The conservation of all Casimirs, Eq. (5), is therefore equivalent to the conservation of $D(\sigma)$.

The conservation of the distribution of vorticity levels, as proven above, can also be understood from the equations of motion. We find that $Dq/Dt = 0$, showing that the values of the potential vorticity field are Lagrangian tracers. This means that the values of q are transported through the non-divergent velocity field, thus keeping the distribution unchanged.

From now on, we restrict ourselves to a K-level vorticity distribution. We make this choice for pedagogical reasons, but a generalization of the discussion of next section to a continuous vorticity distribution is straightforward. The K-level vorticity distribution is defined as

$$D(\sigma) = \sum_{k=1}^{K} A_k \delta(\sigma - \sigma_k), \tag{8}$$

where A_k denotes the area occupied by the vorticity value σ_k. The areas A_k are not arbitrary, their sum is the total area $\sum_{k=1}^{K} A_k = |\mathscr{D}|$. Moreover, the constraint (6), imposes the constraint $\sum_{k=1}^{K} A_k \sigma_k = 0$.

3 Equilibrium statistical mechanics and the mean field variational problem as a large deviation result

3.1 Large deviation theory in 2D turbulence, the equilibrium mean field variational problem

The first large deviation results in two-dimensional turbulence have been obtained in the context of the theory for the 2D Euler equations. Michel and Robert [44] have studied the large deviation of Young measures and have suggested that the entropy of the Miller–Robert–Sommeria theory is the analogue of a large deviation rate function. By considering a prior distribution for the vorticity invariants, in a framework where the invariants are considered in a canonical ensemble rather than in a microcanonical one, Boucher and collaborators [5] have given a derivation of a large deviation result based on finite dimensional approximations of the vorticity field. The beginning of the nineties has also been a time of intense study of the statistical mechanics of the point vortex model [18, 38, 39, 27, 28, 4], a special class of solution of the two-dimensional Euler equations. Among those study, large deviations results for the equilibrium measures where also obtained.

The aim of this section is to present a heuristic construction of microcanonical invariant measures for the 2D Euler equations. This construction primarily follows the initial ideas of the previous works [44, 5], but is much simplified. Moreover, for pedagogical reasons, the reading of this heuristic presentation does not imply any knowledge of large deviation theory and avoids any technical discussion. These measures are constructed using finite dimensional approximation of the vorticity field, with N^2 number of degrees of freedom. N^2 is then the large deviation parameter and the entropy appears as the analogue of the large deviation rate function.

In order to state the main result, let us define $p(\mathbf{r},\sigma)$ as the local probability to observe vorticity values equal to σ at point $\mathbf{r}$: $p(\mathbf{r},\sigma) = \langle \delta(\omega(\mathbf{r}) - \sigma)\rangle$, where δ is the Dirac delta function (we consider averaging $\langle\cdot\rangle$ over the microcanonical measure, see section 3.2). We also define $\overline{\omega}(\mathbf{r}) = \int \mathrm{d}\sigma\, \sigma p(\mathbf{r},\sigma)$ the local vorticity average. Then the large deviation rate function for $p(\mathbf{r},\sigma)$ is $S(E_0) - S[p,E_0]$ where

$$S[p,E_0] = \mathscr{S}[p] \equiv \int_{\mathscr{D}} \sum_k p_k \log p_k \,\mathrm{d}\mathbf{r} \tag{9}$$

if the constraints $\mathscr{N}[p] = 1$, $\forall k$, $A[p_k] = A_k$ and $\mathscr{E}[\overline{\omega}] = E_0$ are satisfied, and $S[p,E_0] = -\infty$ otherwise, and where

$$S(E_0) = \sup_{\{p \,|\, \mathscr{N}[p]=1\}} \{\mathscr{S}[p] \mid \mathscr{E}[\bar{\omega}] = E_0, \forall k\, A[p_k] = A_k\}, \tag{10}$$

with E_0, A_k and $\mathscr{N}$, the energy, the vorticity distribution, and the probability normalization defined in section 3.3 respectively.

The interpretation of this result is that the most probable value for the local probability is the maximizer of the variational problem (10), and that the probability to

observe a departure from this most probable state is exponentially large, with parameter N^2 and rate function (9). Furthermore, the classical mean field equation for the streamfunction ψ can be derived from (9), as discussed in reference [6].

In next sections, we define precisely the microcanonical measure for the 2D Euler equations (section 3.2) and prove that the entropy $S[p,E_0]$ is a large deviation rate function for p (section 3.3). This justifies the mean field variational problem (10).

3.2 Microcanonical measure

In order to properly construct a microcanonical measure, we discretize the vorticity field on a uniform grid with N^2 grid points, define a measure on the corresponding finite-dimensional space and take the limit $N \to \infty$. A uniform grid has to be chosen in order to comply with a formal Liouville theorem for the 2D Euler equations [14, 59].

We denote the lattice points by $\mathbf{r}_{ij} = \left(\frac{i}{N}, \frac{j}{N}\right)$, with $0 \leq i,j \leq N-1$ and denote $\omega_{ij} \equiv \omega(\mathbf{r}_{ij})$ the vorticity value at point $\mathbf{r}_{ij}$. The total number of points is N^2.

As discussed in the previous section, we assume $D(\sigma) = \sum_{k=1}^{K} A_k \delta(\sigma - \sigma_k)$. For this finite-$N$ approximation, our set of microstates (configuration space) is then

$$X_N = \left\{ \omega^N = (\omega_{ij})_{0\leq i,j\leq N-1} \mid \forall i,j\ \omega_{ij} \in \{\sigma_1,\ldots,\sigma_K\},\ \text{and}\ \forall k\ \#\left\{\omega_{ij} \mid \omega_{ij} = \sigma_k\right\} = N^2 A_k \right\}.$$

Here, $\#(A)$ is the cardinal of set A. We note that X_N depends on $D(\sigma)$ through A_k and σ_k (see (8)).

Using the above expression we define the energy shell $\Gamma_N(E_0,\Delta E)$ as

$$\Gamma_N(E_0,\Delta E) = \left\{ \omega^N \in X_N \mid E_0 \leq \mathscr{E}_N\left[\omega^N\right] \leq E_0 + \Delta E \right\},$$

where

$$\mathscr{E}_N = \frac{1}{2N^2} \sum_{i,j=0}^{N-1} \mathbf{v}_{ij}^2 = -\frac{1}{2N^2} \sum_{i,j=0}^{N-1} \omega_{ij}\psi_{ij},$$

is the finite-N approximation of the system energy, with $\mathbf{v}_{ij} = \mathbf{v}(\mathbf{r}_{ij})$ and $\psi_{ij} = \psi(\mathbf{r}_{ij})$ being the discretized velocity field and streamfunction field, respectively. ΔE is the width of the energy shell. Such a finite width is necessary for our discrete approximation, as the cardinal of X_N is finite. Then the set of accessible energies on X_N is also finite. Let $\Delta_N E$ be the typical difference between two successive achievable energies. We then assume that $\Delta_N E \ll \Delta E \ll E_0$. The limit measure defined below is expected to be independent of ΔE in the limit $N \to \infty$.

The fundamental assumption of statistical mechanics states that each microstate in the configuration space is equiprobable. By virtue of this assumption, the probability to observe any microstate is $\Omega_N^{-1}(E_0,\Delta E)$, where $\Omega_N(E_0,\Delta E)$ is the number of accessible microstates, i.e. the cardinal of the set $\Gamma_N(E_0,\Delta E)$. The finite-N specific Boltzmann entropy is defined as

$$S_N(E_0,\Delta E) = \frac{1}{N^2}\log\ \Omega_N(E_0,\Delta E). \tag{11}$$

The microcanonical measure is then defined through the expectation values of any observable A. For any observable $A[\omega]$ (for instance a smooth functional of the vorticity field), we define its finite-dimensional approximation by $A_N\left[\omega^N\right]$. The expectation value of A_N for the microcanonical measure reads

$$\left\langle \mu_N(E_0,\Delta E), A_N\left[\omega^N\right]\right\rangle_N \equiv \left\langle A_N\left[\omega^N\right]\right\rangle_N \equiv \frac{1}{\Omega_N(E_0,\Delta E)}\sum_{\omega^N\in\Gamma_N(E_0,\Delta E)} A_N\left[\omega^N\right].$$

The microcanonical measure μ for the 2D Euler equation is defined as a limit of the finite-N measure:

$$\langle \mu(E_0), A[\omega]\rangle \equiv \lim_{N\to\infty}\left\langle \mu_N(E_0,\Delta E), A_N\left[\omega^N\right]\right\rangle_N.$$

The specific Boltzmann entropy is then defined as

$$S(E_0) = \lim_{N\to\infty} S_N(E_0,\Delta E). \tag{12}$$

3.3 The mean field variational problem as a large deviation result

Computing the Boltzmann entropy by direct evaluation of Eq. (12) is usually an intractable problem. However, we shall proceed in a different way and show that this alternative computation yields the same entropy in the limit $N\to\infty$. We give heuristic arguments in order to prove that the computation of the Boltzmann entropy Eq. (12) is equivalent to the maximization of the constrained variational problem (10) (called a mean field variational problem). This variational problem is the foundation of the RSM approach to the equilibrium statistical mechanics for the 2D Euler equations. The essential message is that the entropy computed from the mean field variational problem (10) and from Boltzmann's entropy definition (12) are the equal in the limit $N\to\infty$. The ability to compute the Boltzmann entropy through this type of variational problems is one of the cornerstones of statistical mechanics.

Our heuristic derivation is based on the same type of combinatorics arguments as the ones used by Boltzmann for the interpretation of its H function in the theory of relaxation to equilibrium of a dilute gas. This derivation doesn't use the technicalities of large deviation theory. The aim is to actually obtain the large deviation interpretation of the entropy and to provide a heuristic understanding using basic mathematics only. The modern mathematical proof of the relationship between the Boltzmann entropy and the mean field variational problem involves Sanov theorem.

Macrostates are set of microscopic configurations sharing similar macroscopic behaviors. Our aim is to properly identify macrostates that fully describe the main features of the largest scales of 2D turbulent flow, and then to compute their probability or entropy.

Let us first define macrostates through local coarse-graining. We divide the $N\times N$ lattice into $(N/n)\times(N/n)$ non-overlapping boxes each containing n^2 grid points (n is an even number, and N is a multiple of n). These boxes are centered on sites $(i,j)=(In,Jn)$, where integers I and J verify $0\le I,J\le N/n-1$. The indices (I,J) label the boxes.

For any microstate $\omega^N\in\Gamma_N$, let f_{IJ}^k be the frequency to find the value σ_k in the box (I,J)

$$F_{IJ}^k(\omega^N)=\frac{1}{n^2}\sum_{i=I-n/2+1}^{I+n/2}\sum_{j=J-n/2+1}^{J+n/2}\delta_{\rm d}(\omega_{ij}-\sigma_k),$$

where $\delta_{\rm d}(x)$ is equal to one whenever $x=0$, and zero otherwise. We note that for all (I,J), $\sum_{k=1}^K F_{IJ}^k(\omega^N)=1$.

A macrostate $p_N=\left\{p_{IJ}^k\right\}_{0\le I,J\le N/n-1;1\le k\le K}$, is the set of all microstates of $\omega^N\in X_N$ such that $F_{IJ}^k(\omega^N)=p_{IJ}^k$ for all I,J, and k (by abuse of notation, and for simplicity, $p_N=\left\{p_{IJ}^k\right\}_{0\le I,J\le N/n-1;1\le k\le K}$ refers to both the set of values and to the set of microstates having the corresponding frequencies). The entropy of the macrostate is defined as the logarithm of the number of microstates in the macrostate

$$S_N[p_N]=\frac{1}{N^2}\log\left(\#\left\{\omega^N\in X_N\;\middle|\;\text{for all } I,J,\text{ and } k,\ F_{IJ}^k(\omega^N)=p_{IJ}^k\right\}\right). \qquad (13)$$

Following an argument by Boltzmann, it is a classical exercise in statistical mechanics, using combinatorics and the Stirling formula, to prove that in the limit $N\gg n\gg 1$, without taking into account of the area constraints A_k, the entropy of the macrostate would converge to

$$S_N[p_N]\overset{N\gg n\gg 1}{\sim}\mathscr{S}_N[p_N]=-\frac{n^2}{N^2}\sum_{I,J=0}^{N/n-1}\sum_{k=1}^{K}p_{IJ}^k\log\,p_{IJ}^k$$

if $\forall I,J,\ \mathscr{N}[p_{IJ}]=1$, and $S_N[p_N]\sim-\infty$ otherwise, where $\mathscr{N}[p_{IJ}]\equiv\sum_k p_{IJ}^k$. The area constraints are easily expressed as constraints over p_N: $A_N\left[p_N^k\right]\equiv\frac{n^2}{N^2}\sum_{I,J=0}^{N/n-1}p_{IJ}^k=A_k$ and $\forall I,J,\ \mathscr{N}[p_{IJ}]=1$. An easy generalization of the above formula gives

$$S_N[p_N]\overset{N\gg n\gg 1}{\sim}\mathscr{S}_N[p_N]$$

if $\forall k$, $A_N\left[p_N^k\right]=A_k$, and $S_N[p_N]\sim-\infty$ otherwise. In the theory of large deviation, this result could have been obtained using Sanov's theorem. We now consider a new macrostate (p_N,E_0) which is the set of microstates ω^N with energy $\mathscr{E}_N\left[\omega^N\right]$ verifying $E_0\le\mathscr{E}_N\left[\omega^N\right]\le E_0+\Delta E$ (the intersection of $\Gamma_N(E_0,\Delta E)$ and p_N). For a given macrostate p_N, not all microstates have the same energy. The constraint on the energy thus can not be recast as a simple constraint on the macrostate p_N. Then one has to treat the energy constraint in a more subtle way. The energy is

$$\mathscr{E}_N\left[\omega^N\right] = -\frac{1}{2N^2}\sum_{i,j=0}^{N-1}\omega_{ij}^N\psi_{ij}^N.$$

The streamfunction ψ_{ij}^N is related to ω^N through

$$\psi_{ij} = \frac{1}{N^2}\sum_{i',j'=0}^{N-1} G_{ij,i'j'}\omega_{i'j'}^N,$$

where $G_{ij,i'j'}$ is the Laplacian Green function in the domain $\mathscr{D}$. In the limit $N \gg n \gg 1$, the variations of $G_{ij,i'j'}$ for (i',j') running over the small box (I,J) are vanishingly small. Then $G_{ij,i'j'}$ can be well approximated by their average value over the boxes $G_{IJ,I'J'}$. Then

$$\psi_{ij} \simeq \psi_{IJ} \equiv \frac{1}{N^2}\sum_{I',J'=0}^{N/n-1} G_{IJ,I'J'}\sum_{i'=I-n/2+1}^{I+n/2}\sum_{j'=J-n/2+1}^{J+n/2}\omega_{i'j'}^N = \frac{n^2}{N^2}\sum_{I',J'=0}^{N-1} G_{IJ,I'J'}\overline{\omega_{IJ}^N},$$

where the coarse-grained vorticity is defined as

$$\overline{\omega_{IJ}^N} = \frac{1}{n^2}\sum_{i'=I-n/2+1}^{I+n/2}\sum_{j'=J-n/2+1}^{J+n/2}\omega_{i'j'}^N.$$

We note that, over the macrostate p_N, the coarse-grained vorticity depends on p_N only:

$$\overline{\omega_{IJ}^N} = \sum_{k=1}^{K} p_{IJ}^k\sigma_k \text{ for } \omega^N \in p_N.$$

Using similar arguments, it is easy to conclude that in the limit $N \gg n \gg 1$ the energy of any microstate of the macrostate p_N is well approximated by the energy of the coarse-grained vorticity

$$\mathscr{E}_N\left[\omega^N\right] \overset{N\gg n\gg 1}{\sim} \mathscr{E}_N\left[\overline{\omega_{IJ}^N}\right] = -\frac{n^2}{2N^2}\sum_{I,J=0}^{N/n-1}\overline{\omega_{IJ}^N}\psi_{IJ}^N.$$

Then the Boltzmann entropy of the macrostate is

$$S_N[p_N,E_0] \overset{N\gg n\gg 1}{\sim} \mathscr{S}_N[p_N] \tag{14}$$

if $\forall k$, $\mathscr{N}[p_N^k] = 1$, $A_N\left[p_N^k\right] = A_k$ and $\mathscr{E}_N\left[\overline{\omega_{IJ}^N}\right] = E_0$, and $S_N[p_N,E_0] \sim -\infty$ otherwise.

Consider $P_{N,E_0}(p_N)$ to be the probability density to observe the macrostate p_N in the finite-N microcanonical ensemble with energy E_0. By definition of the microcanonical ensemble of the entropy $S_N(E_0)$ (see Eq. (11) and the preceding paragraph), we have

$$\log P_{N,E_0}(p_N) \overset{N\to\infty}{\sim} N^2 \left[S_N[p_N,E_0] - S_N(E_0)\right]. \tag{15}$$

From the general definition of a large deviation result given by Eq. (1), we clearly see that formula (14) is a large deviation result for the macrostate p_N in the microcanonical ensemble. The large deviation parameter is N^2 and the large deviation rate function is $-S_N[p_N,E_0]+S_N(E_0)$.

We now consider the continuous limit. The macrostates p_N^k are now seen as the finite-N approximation of p_k, the local probability to observe $\omega(\mathbf{r})=\sigma_k$: $p_k(\mathbf{r}) = \langle\delta(\omega(\mathbf{r})-\sigma_k)\rangle$. The macrostate is then characterized by $p=\{p_1,\dots,p_K\}$. Taking the limit $N\gg n\gg 1$ allows us to define the entropy of the macrostate (p,E_0) as

$$S[p,E_0] = \mathscr{S}[p] \equiv \sum_k \int_{\mathscr{D}} p_k \log p_k \,\mathrm{d}\mathbf{r} \tag{16}$$

if $\forall k\ \mathscr{N}[p_k]=1$, $A[p_k]=A_k$ and $\mathscr{E}[\overline{\omega}]=E_0$, and $S[p,E_0]=-\infty$ otherwise. In the same limit, it is clearly seen from definition (13) and result (16) that there is a concentration of microstates close to the most probable macrostate. The exponential concentration close to this most probable state is a large deviation result, where the entropy appears as the opposite of a large deviation rate function (up to an irrelevant constant).

The exponential convergence towards this most probable state also justifies the approximation of the entropy with the entropy of the most probable macrostate. Thus, in the limit $N\to\infty$ we can express the Boltzmann entropy, Eq. (12), as

$$S(E_0) = \sup_{\{p\,|\,\mathscr{N}[p]=1\}} \left\{\mathscr{S}[p] \;|\; \mathscr{E}[\bar{\omega}]=E_0, \forall k\, A[p_k]=A_k\right\}, \tag{17}$$

where $p=\{p_1,\dots,p_K\}$ and $\forall\ \mathbf{r}$, $\mathscr{N}[p](\mathbf{r}) = \sum_{k=1}^K p_k(\mathbf{r}) = 1$ is the local normalization. Furthermore, $A[p^k]$ is the area of the domain corresponding to the vorticity value $\omega=\sigma_k$. The fact that the Boltzmann entropy $S(E_0)$ Eq. (12) can be computed from the variational problem (17) is a powerful non-trivial result of large deviation theory.

3.4 Applications of equilibrium statistical mechanics

In the two previous sections, we have defined the microcanonical measure for the two-dimensional Euler and quasi geostrophic equations, and we have proven that the logarithm of the probability of a macrostate p is given by the macrostate entropy (16). We can conclude that most of the microstates will correspond to the most probable macrostate, the one that actually maximize the variational problem (17). This most probable macrostate is called the equilibrium macrostate. This means that if we take a random microstate, it will nearly surely have the same velocity as the one of the equilibrium macrostate. As a consequence, we conclude that equilib-

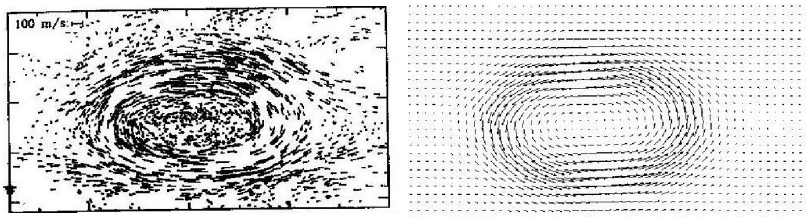

Fig. 5 Left: the observed velocity field is from Voyager spacecraft data, from Dowling and Ingersoll [25] ; the length of each line is proportional to the velocity at that point. Note the strong jet structure of width of order R, the Rossby deformation radius. Right: the velocity field for the statistical equilibrium model of the Great Red Spot. The actual values of the jet maximum velocity, jet width, vortex width and length fit with the observed ones. The jet is interpreted as the interface between two phases; each of them corresponds to a different mixing level of the potential vorticity. The jet shape obeys a minimal length variational problem (an isoperimetrical problem) balanced by the effect of the deep layer shear.

rium macrostates are natural candidates to model self organized large scale turbulent flows, like for instance the Great Red Spot of Jupiter shown on figure (1).

A number of works have considered the comparison of self-organized turbulent flows with equilibrium macrostates. Interested readers will find comparison with experiments and numerical simulations described in the review [64], whereas models of geophysical flows, for instance the Great Red Spot of Jupiter, ocean mesoscale vortices, strong mid basin jets similar to the Gulf Stream or the Kuroshio are discussed in the review [16]. Recent applications to model the vertical structure of oceans can be found in the papers [71, 70].

As an example, figure 5 shows the comparison of the observed velocity field for the Great Red Spot of Jupiter with the velocity field of an equilibrium macrostate of the quasi-geostrophic model. The theoretical analysis of this equilibrium macrostate [11] is based on an analogy with Van Der Walls–Cahn–Hilliard model of first order transition and the shape of the strong jet obeys a minimal length variational problem (an isoperimetrical problem) balanced by the effect of the deep layer shear (see [16] for more details).

Another example of equilibrium prediction is the phase diagram of statistical equilibria for the two-dimensional Euler equation on a doubly periodic domain (torus). This phase diagram (figure 3.4) shows that the statistical equilibria are either dipoles (one cyclone and one anticyclone) or parallel flows. This example is further discussed in the work [10] and the review [16]. This equilibrium phase diagram has also been used in order to predict non-equilibrium phase transitions [10] as is discussed in section 4.4.

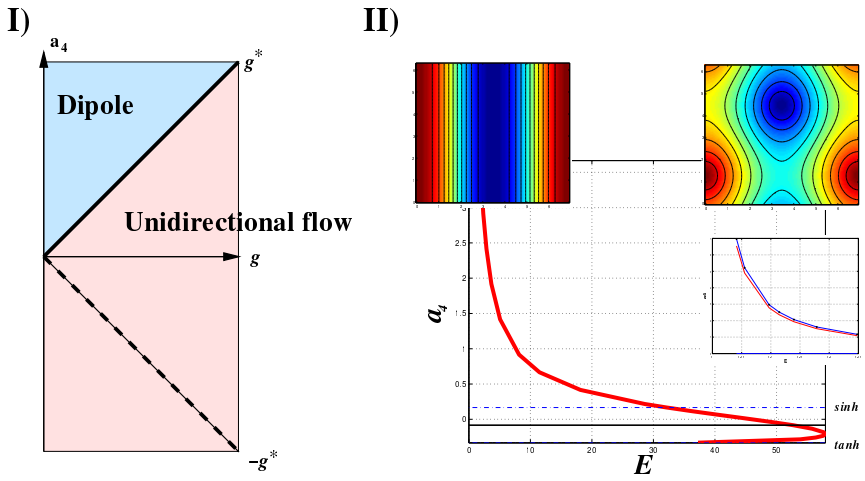

Fig. 6 Bifurcation diagrams for statistical equilibria of the two-dimensional Euler equations in a doubly periodic domain a) in the g-a_4 plane, g is related to the domain aspect ratio and a_4 to the fourth order moment of the vorticity distribution (please see [16]). b) obtained numerically in the $E-a_4$ plane, E is the energy, in the case of doubly periodic geometry with aspect ratio $\delta = 1.1$. The colored insets are streamfunction and the inset curve illustrates good agreement between numerical and theoretical results in the low energy limit.

4 Non equilibrium phase transitions, path integrals, and instanton theory

The aim of this section is to discuss non-equilibrium phase transitions in turbulent flows, more specifically for the dynamics of the two-dimensional Navier–Stokes equations with random forces, quasi-geostrophic dynamics with random forces, or related dynamics. We want to discuss simple examples for which situations with rare transitions between two attractors exist (bistability). We will use path integrals and large deviations in order to compute the most-probable paths for those transitions and the transition rates.

In order to give a pedagogical presentation of path integrals and large deviation theory for stochastic dynamics we first discuss the extremely classical case of the Kramer problem: the over-damped dynamics of a particle in a double-well potential, in section 4.1. We generalize these results to an abstract set of dynamics, called Langevin dynamics, in section 4.2. We apply these results to two-dimensional Euler and Quasi-Geostrophic Langevin dynamics in section 4.3, for which we are able to predict bistability, compute transition rates and the most probable transition paths. Finally we discuss path integral approaches and action minimizer for the stochastic Navier-Stokes equations in a non-equilibrium context in section 4.4.

4.1 Large deviations for the overdamped Langevin dynamics

We wish first to give a pedagogical description of large deviation theory in ***non-equilibrium systems***, more specifically for dynamics consisting of stochastic differential equations. Therefore, we begin by applying large deviation theory to a simple academic example of an over-damped particle in a double-well potential (the Kramer problem) where a large deviation result exists. We will show that we can compute the transition rate for the motion of the particle from one well to the other and that the result is an Arrhenius factor (it is proportional to the exponential of the energy barrier height between the two wells). In fact, this is a large deviation result.

This section develops classical ideas. We use the path integral formalism for stochastic processes [52, 74]. Similar results are discussed by mathematicians in the framework of the Freidlin-Wentzell theory [30, 67]. We are much interested by the time-reversal symmetries of the action and its consequence for the symmetry between relaxation and fluctuation paths, and its consequences for the computation of the most probable transition (instanton). Those symmetries are discuss much less often than the other material, but there are also very classical (some people say it dates from Onsager, we do not know exactly).

4.1.1 The overdamped Langevin dynamics

We consider a single overdamped particle in a 1D double-well potential $V(x)$ and subjected to random forces due to a small coupling to a thermal bath. For simplicity we considered the overdamped limit, for which the dynamics of the particle position x is governed by the stochastic differential equation

$$\dot{x} = -\frac{\mathrm{d}V}{\mathrm{d}x} + \sqrt{\frac{2}{\beta}}\eta, \tag{18}$$

where η is a random white noise with a Gaussian distribution characterized by $\mathbf{E}[\eta(t)\eta(t')] = \delta(t-t')$, $V(x)$ is a double well potential (see Fig. 7), and $\beta = 1/k_B T$ where T is the temperature. In the deterministic situation, when $1/\beta = 0$, the particle relaxes to one of the two stable steady states of the potential V, i.e. it converges either to $x = -1$ or to $x = 1$. In the presence of thermal noise, the particle may gain enough energy to jump the potential barrier at $x = 0$ and settle in the other potential well. If the forcing is weak, i.e. $1 \ll \beta\Delta V$, then the jumps between wells will be rare events and will be statistically independent from one another. They will then be described by a Poisson process characterized by a transition rate λ. We will show that one can apply the theory of large deviations in order to compute λ. Moreover the theory of large deviation will lead to the conclusion that most of the transition paths concentrate close to the most probable transition path. As will be discussed more precisely below, this most probable transition path in this situation is called an instanton.

In order to obtain these results, we will use formal computations based on a path integral formulation of the transition probabilities for the stochastic process (18). Such a path integral formulation is referred as Onsager–Machlup formalism, as Onsager and Machlup first proposed it, few years after the path integral formulation of quantum mechanics by Feynman.

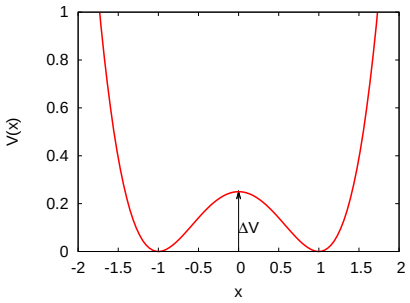

Fig. 7 Graph of the double well potential $V(x) = (x^2-1)^2/4$. We observe two stable steady states at $x = \pm 1$ and a saddle at $x = 0$ with height $\Delta V = 1/4$.

4.1.2 The transition probability as a path integral

To give a simple understanding of the Onsager-Machlup formalism, we first consider a vector $\eta = \{\eta_i\}_{1\le i\le N}$ of independent Gaussian random variables, with zero mean $\mathbf{E}(\eta_i) = 0$ and covariance $\mathbf{E}(\eta_i\eta_j) = \delta_{ij}$. By definition, the probability measure of η is the Gaussian measure

$$\mathrm{d}\mu = \exp\left(-\frac{1}{2}\sum_{i=1}^{N}\eta_i^2\right)\prod_{i=1}^{N}\frac{\mathrm{d}\eta_i}{\sqrt{2\pi}}. \tag{19}$$

The Euler approximation of the Langevin equation (18) is, within the Ito convention,

$$x_i = x_{i-1} - \Delta t\,\frac{\mathrm{d}V}{\mathrm{d}x}(x_{i-1}) + \sqrt{\frac{2\Delta t}{\beta}}\,\eta_i \tag{20}$$

for $1 \le i \le N$ and with $x_0 = x(0)$ a given initial state. The probability measure of a particular path $x = \{x_i\}_{1\le i\le N}$ is given by inverting (20) and inserting it in (19),

$$\mathrm{d}\mu = \exp\left(-\frac{\beta}{4}\sum_{i=1}^{N}\left(\frac{x_i - x_{i-1}}{\Delta t} + \frac{\mathrm{d}V}{\mathrm{d}x}(x_{i-1})\right)^2\Delta t\right)J(\eta\,|x)\prod_{i=1}^{N}\frac{\mathrm{d}x_i}{\sqrt{2\pi}}. \tag{21}$$

In this expression, $J(\eta|x)$ is the Jacobian of the change of variable $\eta \to x$. In the Ito convention (20), the corresponding matrix is lower-triangular with ones in the diagonal, so that $J(\eta|x) = 1$.

The measure of a Gaussian stochastic process $\eta(t)$ of zero mean $\mathbf{E}[\eta(t)] = 0$ and covariance $\mathbf{E}[\eta(t)\eta(t')] = \delta(t-t')$, on a time interval $[0,T]$ with $T = N\Delta t$, is the formal generalization of the above finite dimensional measure (19),

$$\mathrm{d}\mu = \exp\left(-\frac{1}{2}\int_0^T \eta^2(t)\mathrm{d}t\right)\mathscr{D}[\eta]. \tag{22}$$

The differential element $\mathscr{D}[\eta]$ in the above expression is the formal limit of the finite-dimensional quantity $\prod_{i=1}^N \frac{\mathrm{d}\eta_i}{\sqrt{2\pi}}$ for $N \to \infty, \Delta t \to 0$, where $\eta_i = \eta(i\Delta t) = \eta(iT/N)$. People well trained in mathematics know the difficulty to define such an object, but we will keep our discussion at a formal level and state that this formal notation contains all the mathematical subtleties related to the limit $N \to \infty, \Delta t \to 0$. Then, the probability measure of a particular trajectory $\{x(t)\}_{0\le t\le T}$ is also the formal limit of (21),

$$\mathrm{d}\mu = \exp\left(-\frac{\beta}{4}\int_0^T \left(\dot{x} + \frac{\mathrm{d}V}{\mathrm{d}x}\right)^2 \mathrm{d}t\right) J[\eta|x]\mathscr{D}[x], \tag{23}$$

where $J[\eta|x]$ is the Jacobian of the change of variable $\eta \to x$, and is also equal to one (we refer to [74] for a more general treatment, noting that [74] actually use the Stratonovich convention).

The transition probability from an initial state x_0 at time 0 to a final state x_T at time T is the sum over all possible paths $\{x(t)\}_{0\le t\le T}$ such that $x(0) = x_0$ and $x(T) = x_T$ of the probability of a single path (23). Such a sum can be formally written as the path integral

$$P(x_T, T; x_0, 0) = \int_{x(0)=x_0}^{x(T)=x_T} \exp\left(-\frac{\beta}{2}\mathscr{A}[x]\right)\mathscr{D}[x], \tag{24}$$

with the action functional

$$\mathscr{A}[x] = \frac{1}{2}\int_0^T \left(\dot{x} + \frac{\mathrm{d}V}{\mathrm{d}x}\right)^2 \mathrm{d}t. \tag{25}$$

From (24), it is clear that the most probable trajectories with prescribed initial and final states are minimizers of the action with prescribed initial and final point. The optimal action is denoted

$$A(x_0, x_T, T) = \min\left\{\mathscr{A}[x] \,|\, x(0) = x_0, x(T) = x_T\right\}.$$

4.1.3 Fluctuation paths

When the initial point $x_0 = x_a$ belongs to an attractor of the deterministic dynamics (for the Kramer problem, if $x_0 = x_a = \pm 1$ is a stable fixed points), it is expected that the action $A(x_a, X, T)$ decreases with time. The action minima starting from one attractor and having an infinite duration will thus play an important role. Moreover, those infinite time action minimizers are essential because the transition probability $P(X, T; x_a, 0)$ converges to the stationary distribution of the stochastic process when the time T goes to infinity. Those action minimizers starting from one attractor and with an infinite duration are called fluctuation paths, they solve

$$A(x_a, X, \infty) = \min \left\{ \mathscr{A}[x] \,|\, \lim_{T\to\infty} x(-T) = x_a, x(0) = X \right\}.$$

4.1.4 Relaxation paths

We consider a state X that belongs to the basin of attraction of an attractor x_a of the deterministic dynamics. The relaxation path starting at x, denoted $\{x_r(t)\}_{0\le t\le T}$ is defined by

$$\dot{x}_r = -\frac{\mathrm{d}V}{\mathrm{d}x}(x_r)$$

with initial conditions $x_r(0) = X$. As the path converges to x_a, we have $x_r(+\infty) = x_a$. Using the expression of the action (25), we see that $\mathscr{A}[x_r] = 0$, as the relaxation path is a deterministic solution, and we also notice that $\mathscr{A}[x] \ge 0$ for any path $\{x(t)\}_{0\le t\le T}$. As a consequence, relaxation paths are global minimizers of the action $\mathscr{A}[x]$. This is because following the deterministic dynamics x_r in order to reach the attractor x_a starting from X doesn't require any stochastic perturbation, so that the cost is zero and the probability is maximal.

4.1.5 Time-reversal symmetry and the relation between fluctuation and relaxation paths

In order to characterize fluctuations paths and instantons, we will take profit of the time-reversal symmetry of the over-damped Langevin dynamics. We consider a path $\{x(t)\}_{0\le t\le T}$ and the reversed path $R[x] = \{x(T-t)\}_{0\le t\le T}$. The action of the reversed path reads

$$\mathscr{A}[R[x]] = \frac{1}{2}\int_0^T \left(\frac{\mathrm{d}}{\mathrm{d}t}R[x] + \frac{\mathrm{d}V}{\mathrm{d}x}(R[x])\right)^2 \mathrm{d}t = \frac{1}{2}\int_0^T \left(-\dot{x}(t') + \frac{\mathrm{d}V}{\mathrm{d}x}(x(t'))\right)^2 \mathrm{d}t',$$

with the change of variable $t' = T - t$. Then, writing

$$\left(\dot{x} - \frac{\mathrm{d}V}{\mathrm{d}x}\right)^2 = \left(\dot{x} + \frac{\mathrm{d}V}{\mathrm{d}x}\right)^2 - 4\dot{x}\frac{\mathrm{d}V}{\mathrm{d}x} = \left(\dot{x} + \frac{\mathrm{d}V}{\mathrm{d}x}\right)^2 - 4\frac{\mathrm{d}}{\mathrm{d}t}V(x),$$

we get

$$\mathscr{A}[R[x]] = \mathscr{A}[x] - 2\left(V(x(T)) - V(x(0))\right). \tag{26}$$

Plugging this relation into the path integral expression of the transition probability (24), we obtain

$$P(R[x_T],T;R[x_0],0) = P(x_T,T;x_0,0)\exp\left(\frac{V(x(T)) - V(x(0))}{k_B T}\right).$$

We recognize the Gibbs stationary distribution of the over-damped Langevin equation $P_S(x) = \frac{1}{Z}\mathrm{e}^{-V(x)/k_B T}$, so that the above expression gives the detailed balance relation

$$P(x_T,T;x_0,0)P_S(x_0) = P(x_0,T;x_T,0)P_S(x_T).$$

We have thus proven that detailed balance is a consequence of the time-reversal symmetry, as expected on general ground.

We now consider the fluctuation path from one attractor x_a to any point X of its basin of attraction. Using relation (26) and the fact that the action is always positive, we have

$$\mathscr{A}[x] \geq 2\left(V(x(T)) - V(x(0))\right), \tag{27}$$

with equality if and only if x is a minimizer of the reversed action $\mathscr{A}[R[x]]$. If the initial state is an attractor and the final state is another point in the associated basin of attraction, the reversed action $\mathscr{A}[R[x]]$ is naturally minimized by the relaxation path $R[x] = x_r$ that goes from X to the attractor,

$$\frac{\mathrm{d}}{\mathrm{d}t}R[x] = -\frac{\mathrm{d}V}{\mathrm{d}x}(R[x])$$

with $R[x](0) = X$ and $R[x](+\infty) = x_a$. Then the minimizer of $\mathscr{A}[x]$ is the reversed relaxation path. We thus conclude that the fluctuation path from x_a to X, is the time reversed of the relaxation path from X to x_a. This situation is schematically represented in figure 8.

4.1.6 Instanton and large deviation principle

We define the instanton as the most probable path that go from one attractor $x_{-1} = -1$ to the other one $x_1 = 1$ in an infinite time. More precisely we consider x_T the minimizer of the variational problem $\min\left\{\mathscr{A}[x] \,|\, x\left(-\frac{T}{2}\right) = x_{-1} \text{ and } x\left(\frac{T}{2}\right) = x_1\right\}$, and the instanton is the limit when $T \to \infty$ of x_T. The instanton action is

$$A(x_{-1},x_1) = \lim_{T\to\infty} \min\left\{\mathscr{A}[x] \,|\, x\left(-\frac{T}{2}\right) = x_{-1} \text{ and } x\left(\frac{T}{2}\right) = x_1\right\},$$

As will soon become clear, instantons are related to the most probable transition paths, and their action to the transition rate λ.

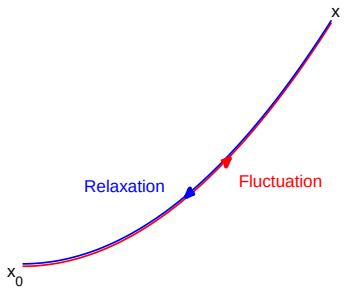

Fig. 8 Schematic representation of the fluctuation and relaxation paths between an attractor of the deterministic dynamics x_0 and another point X in the basin of attraction of x_0, for the over-damped dynamics. The relaxation path is the deterministic trajectory from x to x_0, and the fluctuation path is the time-reversed trajectory. Both trajectories are the most probable paths with the associated initial and final states.

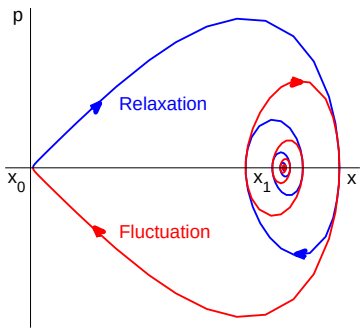

Fig. 9 Fluctuation and relaxation paths between an initial position x_0 and an attractor x_1, for the full Langevin dynamics 30. The fluctuation path (reversed relaxation path) is obtained by reversal of time, so the momentum is changed as $p \to -p$. Both trajectories are the most probable paths with the associated initial and final conditions.

From the previous discussion, it is easily understood that instantons are decomposed into two parts. First, there is the fluctuation path from x_{-1} to the saddle $x_s = 0$, which is the reverse of the relaxation path from x_s to x_{-1}. The action of this part of the trajectory is given by (26), it is $\mathscr{A}[R[x_r]] = 2\,(V(x_s) - V(x_{-1})) = 2\Delta V$, where ΔV is the potential barrier height. The second part of the instanton trajectory is the relaxation path from the saddle x_s to the final attractor x_1. The action of this relaxation path is zero, so that the total instanton action is $\mathscr{A}[x^*] = 2\Delta V$.

A more precise analysis shows that as both the fluctuation path to the saddle and the relaxation path last for an infinite time (an infinite time is needed to quit the attractor and an infinite time is needed to reach the saddle). This explains the definition of the instanton through the limit of the finite time minimizer x_T. One can also understand that any temporal translation of an instanton is another minimizer from on attractor $x_{-1} = -1$ to the other one $x_1 = 1$ in an infinite time. This degeneracy is related to the notion of a "free-instanton-molecule" gas approximation and has the consequence that for time $T \gg 1$, the transition probability is proportional to time T:

$$P(x_1, T; x_{-1}, 0) \overset{T\gg 1}{\sim} \lambda T.$$

We refer to [19] for a detailed discussion.

In the limit of small forcing $1 \ll \beta\Delta V$, the distribution given by the path integral (24) is concentrated around its most probable state, the instanton we have determined. We can thus apply a saddle-point approximation in order to get the transition probability P_t,

$$\lim_{\beta\to\infty} -\frac{1}{\beta}\log(P_t) = \Delta V. \tag{28}$$

Formula (28) states that the transition probability for observing the rare transition between the two potential wells, in the limit of the weak noise limit, is proportional to the exponential of the barrier height ΔV. Such a result is called a large deviation principle for the probability P_t. We recover the exponential factor of the Arrhenius formula for the transition rate

$$\lambda = \frac{1}{\tau}\exp\left(-\frac{\Delta V}{k_B T}\right) \tag{29}$$

where ΔV is the energy barrier height and $k_B T$ is the temperature.

The computation of the prefactor $1/\tau$ goes beyond a large deviation result. It was already computed by Kramer, for an overdamped Kramer dynamics. It was the subject of Langer theory for systems with many degrees of freedom. Alternatively, it can be computing in the path integral framework by computing the path integrals at next order, computing the properties of the Gaussian processes close to the instanton, and treating correctly the subtleties related to the instanton degeneracy due to time translation. Such a computation can be found for example in the reference [19]. The result is

$$\tau = 2\pi\left(\frac{d^2V}{dx^2}(x_0)\frac{d^2V}{dx^2}(x_{-1})\right)^{-1/2}.$$

4.1.7 Generalization to the inertial Langevin dynamics

We consider now the dynamics of a particle in the same double-well potential, with random forces, but without the over-damped approximation. The position and momentum of the particle $\{x,p\}$ satisfy

$$\begin{cases} \dot{x} = p \\ \dot{p} = -\frac{\mathrm{d}V}{\mathrm{d}x} - \alpha p + \sqrt{\frac{2\alpha}{\beta}}\eta. \end{cases} \tag{30}$$

In this case, the time-reverse of a given path $\{x(t),p(t)\}_{0\le t\le T}$ is given by $I[x,p] = \{x(T-t),-p(T-t)\}_{0\le t\le T}$, as represented in figure 9. It is easily proven that the action of the reversed action path satisfies a relation similar to 26. Then, as in the overdamped case, one easily proves that the fluctuation paths is the time reverse of the relaxation paths. As in the over-damped case, instantons from one attractor to the other are composed of a fluctuation path (time reversed relaxation path) from the first attractor $\{x_{-1}=-1,p_{-1}=0\}$ to the saddle $\{0,0\}$, and a relaxation path from the saddle to the final attractor $\{1,0\}$.

4.2 Langevin dynamics with potential $\mathscr{G}$

The aim of this section is to generalize the results discussed for the Kramer model in section 4.1 to a class of dynamics that corresponds to systems coupled with equilibrium (thermal) baths. The consider dynamics with Liouville theorem (for instance Hamiltonian dynamics), with dissipation which are the gradient of a conserved quantity and stochastic forces with Einstein type relations. For those Langevin dynamics, we prove detailed balance (sometimes in a generalized form), we prove that the fluctuation paths are the time reversed of the relaxation paths, and we describe the instantons.

Whereas such Langevin dynamics are very common in physics, the discussion below is original. As far as we know we are the first to describe this general framework, especially for the case when the potential is not the Hamiltonian but another conserved quantity. The aim is to apply this framework to dynamics that include the two-dimensional Euler and quasi-gestrophic dynamics.

4.2.1 Definition of Langevin dynamics

In this section we consider the deterministic dynamics

$$\frac{\partial q}{\partial t} = \mathscr{F}[q] \tag{31}$$

where q is either a finite dimensional variable or a field.

If $q \in \mathbf{R}^N$, the dynamics is $\frac{\partial q_i}{\partial t} = \mathscr{F}_i[q]$. We then assume that this dynamical system conserves the Liouville measure $\prod_{i=1}^N \mathrm{d}q_i$, or equivalently that the divergence of the vector field $\mathscr{F}$ is zero

$$\nabla.\mathscr{F} \equiv \sum_{i=1}^{N} \frac{\partial \mathscr{F}_i}{\partial q_i} = 0.$$

We call this property a Liouville theorem.

If q is a field (for instance a two-dimensional vorticity or potential vorticity field), defined over a domain $\mathscr{D}$, $\mathscr{F}[q](\mathbf{r})$ is a quantity computed from the field q at any point $\mathbf{r}$. For instance for the Quasi-Geostrophic equation $\mathscr{F}[q] = -\mathbf{v}[q-h]\cdot\nabla q(\mathbf{r})$. We continue the discussion for a field equation only. For any functional $\mathscr{K}$, $\frac{\delta \mathscr{K}}{\delta q(\mathbf{r})}$ is the functional derivative of $\mathscr{K}$ at point $\mathbf{r}$, a generalization of the usual derivative, such that for any variation δq, at linear order the first variations of $\mathscr{K}$ are given by

$$\delta \mathscr{K} = \int_{\mathscr{D}} \frac{\delta \mathscr{K}}{\delta q(\mathbf{r})} \delta q(\mathbf{r})\, \mathrm{d}\mathbf{r}.$$

We assume that a Liouville theorem holds for the dynamics (31), in the sense that the formal generalization of the finite dimensional Liouville theorem

$$\nabla.\mathscr{F} \equiv \int_{\mathscr{D}} \frac{\delta \mathscr{F}}{\delta q(\mathbf{r})}(\mathbf{r})\, \mathrm{d}\mathbf{r} = 0,$$

is verified.

We also assume that this dynamical system has a conserved quantity $\mathscr{G}$: $\mathrm{d}\mathscr{G}/\mathrm{dt} = 0$. From (31), we see that this is equivalent to

$$\int_{\mathscr{D}} \mathscr{F}[q](\mathbf{r}) \frac{\delta \mathscr{G}}{\delta q(\mathbf{r})}[q]\, \mathrm{d}\mathbf{r} = 0, \tag{32}$$

for any q. Those hypothesis are verified, for instance if the dynamical system is an Hamiltonian system

$$\mathscr{F}(q) = \{q, \mathscr{H}\},$$

where $\{.,.\}$ is a Poisson bracket, and $\mathscr{G}$ one of the conserved quantity of the Hamiltonian system, for instance $\mathscr{G} = \mathscr{H}$. We stress however that $\mathscr{G}$ does not need to be $\mathscr{H}$.

If the Liouville hypothesis is verified and $\mathscr{G}$ is a conserved quantity, we call a Langevin dynamics for the potential $\mathscr{G}$ the stochastic dynamics

$$\frac{\partial q}{\partial t} = \mathscr{F}[q](\mathbf{r}) - \alpha \int_{\mathscr{D}} C(\mathbf{r},\mathbf{r}') \frac{\delta \mathscr{G}}{\delta q(\mathbf{r}')}[q]\, \mathrm{d}\mathbf{r}' + \sqrt{2\alpha\gamma}\eta, \tag{33}$$

where we have introduced a stochastic force η, which we assume to be a Gaussian process, white in time, and correlated as $\mathbf{E}[\eta(\mathbf{r},t)\eta(\mathbf{r}',t')] = C(\mathbf{r},\mathbf{r}')\delta(t-t')$. As it is a correlation function, C has to be a symmetric positive function: for any function ϕ over $\mathscr{D}$

$$\int_{\mathscr{D}}\int_{\mathscr{D}} \phi(\mathbf{r}) C(\mathbf{r},\mathbf{r}') \phi(\mathbf{r}')\, \mathrm{d}\mathbf{r}\mathrm{d}\mathbf{r}' \geq 0, \tag{34}$$

and $C(\mathbf{r},\mathbf{r}') = C(\mathbf{r}',\mathbf{r})$. For simplicity, we assume in the following that C is positive definite and has an inverse C^{-1} such that

$$\int_{\mathscr{D}} C(\mathbf{r},\mathbf{r}_1) C^{-1}(\mathbf{r}_1,\mathbf{r}')\mathrm{d}\mathbf{r}_1 = \delta(\mathbf{r}-\mathbf{r}').$$

The major property of a Langevin dynamics is that the stationary probability density functional is known a-priori. It is

$$P_s[q] = \frac{1}{Z}\exp\left(-\frac{\mathscr{G}[q]}{\gamma}\right),$$

where Z is a normalization constant. At a formal level, this can be checked easily by writing the Fokker-Planck equation for the evolution of the probability functionals. Then the fact that P_s is stationary readily follows from the Liouville theorem and the property that $\mathscr{G}$ is a conserved quantity for the deterministic dynamics.

4.2.2 Reversed Langevin dynamics

We consider I a linear involution on the space of fields q (I is a linear functional with $I^2 = \mathrm{Id}$). We define the reversed Langevin dynamics with respect to I as

$$\frac{\partial q}{\partial t} = \mathscr{F}_r[q](\mathbf{r}) - \alpha \int_{\mathscr{D}} C_r(\mathbf{r},\mathbf{r}') \frac{\delta \mathscr{G}_r}{\delta q(\mathbf{r}')}[q]\,\mathrm{d}\mathbf{r}' + \sqrt{2\alpha\gamma}\eta, \tag{35}$$

where

$$\mathscr{F}_r = -I \mathrm{o} \mathscr{F} \mathrm{o} I, \tag{36}$$

$$C_r = I^+ C I, \tag{37}$$

where I^+ is the adjoint of I for the L^2 scalar product and

$$\mathscr{G}_r[q] = \mathscr{G}[I[q]]. \tag{38}$$

From the properties of $\mathscr{F}$, C and $\mathscr{G}$, one can easily check that the Liouville theorem holds for $\mathscr{F}_r$, that C_r is definite positive and that $\mathscr{G}_r$ is a conserved quantity for the dynamics $\frac{\partial q}{\partial t} = \mathscr{F}_r[q]$: for any q

$$\int_{\mathscr{D}} \mathscr{F}_r[q](\mathbf{r}) \frac{\delta \mathscr{G}_r}{\delta q(\mathbf{r})}[q]\,\mathrm{d}\mathbf{r} = 0. \tag{39}$$

As a consequence, the reversed Langevin dynamics (35) is actually a Langevin dynamics too.

A very interesting case, is when the deterministic dynamics is symmetric with respect to time reversal. Then it exists a linear involution I such that

$$\mathscr{F} = \mathscr{F}_r = -I \mathrm{o} \mathscr{F} \mathrm{o} I. \tag{40}$$

If moreover C and $\mathscr{G}$ are symmetric with respect to the involution: $C_r = C$, and

$$\mathscr{G}_r = \mathscr{G}, \tag{41}$$

then the reversed Langevin dynamics is nothing else than the initial Langevin dynamics itself. We then say that the Langevin dynamics is time-reversible. Simple examples of time reversible Langevin dynamics are the overdamped processes

$$\dot{q} = -\int_{\mathscr{D}} C(\mathbf{r},\mathbf{r}') \frac{\delta \mathscr{G}}{\delta q(\mathbf{r}')}[q]\,\mathrm{d}\mathbf{r}' + \sqrt{2\gamma}\eta,$$

which can be proved to be time reversible with the involution $I = \mathrm{Id}$, or the canonical Langevin dynamics

$$\begin{cases} \dot{x} = p \\ \dot{p} = -\dfrac{\mathrm{d}V}{\mathrm{d}x} - \alpha p + \sqrt{2\alpha k_B T}\eta \end{cases},$$

with $I\begin{pmatrix} x \\ p \end{pmatrix} = \begin{pmatrix} x \\ -p \end{pmatrix}$, or the 2D Euler stochastic Euler equation

$$\frac{\partial \omega}{\partial t} + \mathbf{v}\cdot\nabla\omega = -\alpha \int_{\mathscr{D}} C(\mathbf{r},\mathbf{r}') \frac{\delta \mathscr{G}}{\delta \omega(\mathbf{r}')} \mathrm{d}\mathbf{r}' + \sqrt{2\alpha\gamma}\eta$$

with $\mathscr{G}$ an even conserved quantity ($\mathscr{G}[-\omega] = \mathscr{G}[\omega]$), where one should then use $I[\omega] = -\omega$. But in the following we will need to consider cases when the Langevin dynamics is not time reversible, for instance the 2D-stochastic Euler equations when $\mathscr{G}$ is not even or the quasi-geostrophic equations.

4.2.3 Path integrals, action, and time reversal symmetry.

The Lagrangian $\mathscr{L}$ associated to the Langevin dynamics (33) is defined as

$$\mathscr{L}\left[q, \frac{\partial q}{\partial t}\right] = \frac{1}{2\alpha}\int_{\mathscr{D}}\int_{\mathscr{D}} \left(\frac{\partial q}{\partial t} - \mathscr{F}[q](\mathbf{r}) + \alpha \int_{\mathscr{D}} C(\mathbf{r},\mathbf{r}_1)\frac{\delta \mathscr{G}}{\delta q(\mathbf{r}_1)}[q]\,\mathrm{d}\mathbf{r}_1\right) \times \quad (42)$$

$$C^{-1}(\mathbf{r},\mathbf{r}')\left(\frac{\partial q}{\partial t} - \mathscr{F}[q](\mathbf{r}') + \alpha \int_{\mathscr{D}} C(\mathbf{r}',\mathbf{r}_2)\frac{\delta \mathscr{G}}{\delta q(\mathbf{r}_2)}[q]\,\mathrm{d}\mathbf{r}_2\right)\mathrm{d}\mathbf{r}\mathrm{d}\mathbf{r}', \quad (43)$$

and the action functional as

$$\mathscr{A}[q,T] = \int_0^T \mathscr{L}\left[q(t), \frac{\partial q}{\partial t}(t)\right]\mathrm{d}t. \quad (44)$$

The Lagrangian of the reverse process is defined as

$$\mathscr{L}_r\left[q, \frac{\partial q}{\partial t}\right] = \frac{1}{2\alpha}\int_{\mathscr{D}}\int_{\mathscr{D}} \left(\frac{\partial q}{\partial t} - \mathscr{F}_r[q](\mathbf{r}) + \alpha \int_{\mathscr{D}} C_r(\mathbf{r},\mathbf{r}_1)\frac{\delta \mathscr{G}_r}{\delta q(\mathbf{r}_1)}[q]\,\mathrm{d}\mathbf{r}_1\right) \times \quad (45)$$

$$C_r^{-1}(\mathbf{r},\mathbf{r}')\left(\frac{\partial q}{\partial t} - \mathscr{F}_r[q](\mathbf{r}') + \alpha \int_{\mathscr{D}} C_r(\mathbf{r}',\mathbf{r}_2)\frac{\delta \mathscr{G}_r}{\delta q(\mathbf{r}_2)}[q]\,\mathrm{d}\mathbf{r}_2\right)\mathrm{d}\mathbf{r}\mathrm{d}\mathbf{r}' \quad (46)$$

and the reverse action functional $\mathscr{A}_r$, accordingly.

We now consider the path integral formalism (Onsager-Machlup) introduced in section 4.1, for the Langevin dynamics (33). By a generalization of the discussion in section 4.1, we conclude that the transition probability to go from the state q_0 at time 0 to the state q_T at time T, $P[q_T,T;q_0,0]$, can be expressed as

$$P[q_T,T;q_0,0] = \int_{\left\{ q \,\middle|\, \begin{matrix} q_{(0)} = q_0 \\ q_{(T)} = q_T \end{matrix} \right\}} \mathscr{D}[q]\,\mathrm{e}^{-\frac{\mathscr{A}}{2\gamma}}, \quad (47)$$

where we have used that the Jacobian $J[q] = \left|\det\left[\partial_t q - \alpha\int_{\mathscr{D}} C(\mathbf{r}',\mathbf{r}_2)\frac{\delta\mathscr{G}}{\delta q(\mathbf{r}_2)}[q]\,\mathrm{d}\mathbf{r}_2/q\right]\right|$ is equal to one if we assume Ito convention.

For a given path $\{q(t)\}_{0\leq t\leq T}$, we define the reversed path defined by $q_r(t) = I[q(T-t)]$. The main interest of the reversed process stems from the study of temporal symmetries of the stochastic process and the remark that

$$\mathscr{A}[q_r,T] = \mathscr{A}_r[q,T] - 2\left(\mathscr{G}[q(T)] - \mathscr{G}[q(0)]\right). \tag{48}$$

Equivalently, using (38), we also have

$$\mathscr{A}[q,T] = \mathscr{A}_r[q_r,T] + 2\left(\mathscr{G}[q(T)] - \mathscr{G}[q(0)]\right). \tag{49}$$

Let us prove this equality. Using the definition of $\mathscr{F}_r$, $\mathscr{G}_r$ and C_r (Eqs. (36-38)), that

$$\frac{\delta \mathscr{G}_r}{\delta q(\mathbf{r})}[q] = I\frac{\delta \mathscr{G}}{\delta q(\mathbf{r})}[I[q]],$$

and that $I^2 = \mathrm{Id}$, we have

$$\mathscr{L}\left[I[q], -\frac{\partial}{\partial t}I[q]\right] = \frac{1}{2\alpha}\int_{\mathscr{D}}\int_{\mathscr{D}}\left(\frac{\partial q}{\partial t} - \mathscr{F}_r[q](\mathbf{r}) - \alpha\int_{\mathscr{D}} C_r(\mathbf{r},\mathbf{r}_1)\frac{\delta \mathscr{G}_r}{\delta q(\mathbf{r}_1)}[q]\,\mathrm{d}\mathbf{r}_1\right) \tag{50}$$

$$C_r^{-1}(\mathbf{r},\mathbf{r}')\left(\frac{\partial q}{\partial t} - \mathscr{F}_r[q](\mathbf{r}') - \alpha\int_{\mathscr{D}} C_r(\mathbf{r}',\mathbf{r}_2)\frac{\delta \mathscr{G}_r}{\delta q(\mathbf{r}_2)}[q]\,\mathrm{d}\mathbf{r}_2\right)\mathrm{d}\mathbf{r}\mathrm{d}\mathbf{r}' \tag{51}$$

Then, expanding and using the conservation of $\mathscr{G}_r$ we have

$$\mathscr{L}\left[I[q], -\frac{\partial}{\partial t}I[q]\right] = \mathscr{L}_r\left[q, \frac{\partial q}{\partial t}\right] - 2\int_{\mathscr{D}}\frac{\partial q}{\partial t}\frac{\delta \mathscr{G}}{\delta q(\mathbf{r})}\mathrm{d}\mathbf{r}$$

or equivalently

$$\mathscr{L}\left[I[q], -\frac{\partial}{\partial t}I[q]\right] = \mathscr{L}_r\left[q, \frac{\partial q}{\partial t}\right] - 2\frac{\mathrm{d}}{\mathrm{d}t}\mathscr{G}[q].$$

Using this formula and (44) in order to compute $\mathscr{A}[q_r,T]$, we obtain (48).

Performing the change of variable $q_r(t) = I[q(T-t)]$ in the path integral representation (47), and using the action duality formula (48), we obtain

$$P[q_T,T;q_0,0]\,\mathrm{e}^{-\frac{\mathscr{G}[q_0]}{\gamma}} = P_r[I[q_0],T;I[q_T],0]\,\mathrm{e}^{-\frac{\mathscr{G}_r[I[q_T]]}{\gamma}}, \tag{52}$$

where P_r is a transition probability for the reverse process. We have thus obtain a relation between the transition probabilities of the direct process and the transition probabilities of the reverse one.

4.2.4 Detailed balance for reversible processes

If we assume that the Langevin dynamics is time reversible, then the direct and the reverse processes are the same, and the duality relation for the transition probabilities imply

$$P\left[q_T,T;q_0,0\right]\mathrm{e}^{-\frac{\mathscr{G}[q_0]}{\gamma}}=P\left[I\left[q_0\right],T;I\left[q_T\right],0\right]\mathrm{e}^{-\frac{\mathscr{G}[I[q_T]]}{\gamma}},$$

where it is also true that $\mathrm{e}^{-\frac{\mathscr{G}[I[q_T]]}{\gamma}}=\mathrm{e}^{-\frac{\mathscr{G}[q_T]}{\gamma}}$. This result is the detailed balance property for the stochastic process.

When the reverse process is different from the direct one, we see no reason why detailed balance should be true in general.

4.2.5 Steady states of the deterministic dynamics and critical points of the potential $\mathscr{G}$

Let us prove that any non-degenerate critical point of the potential is also a steady state of the deterministic dynamics. This is a classical result in mechanics: for instance any critical point of the energy, if non degenerate, is a steady state.

The extrema of the stationary PDF are critical points of the potential $\mathscr{G}$. Such a critical point q_c verifies

$$\frac{\delta\mathscr{G}}{\delta q(\mathbf{r})}\left[q_c\right]=0.$$

We assume that the critical point is non-degenerate, that is the second variations of $\mathscr{G}$ have no null eigenvalue: more explicitly, the relation

$$\int_{\mathscr{D}}\frac{\delta^2\mathscr{G}}{\delta q(\mathbf{r})\delta q(\mathbf{r}')}\left[q_c\right]\phi(\mathbf{r}')\,\mathrm{d}\mathbf{r}'=0$$

implies that $\phi=0$. If the critical point is non-degenerate then we can prove that q_c is also a steady state of the Hamiltonian dynamics.

We use that $\mathscr{G}$ is conserved. Computing $\delta/\delta q(\mathbf{r})$ of (32) we obtain that for any q

$$\int_{\mathscr{D}}\frac{\delta^2\mathscr{G}}{\delta q(\mathbf{r}_2)\delta q(\mathbf{r})}\left[q\right]\mathscr{F}\left[q\right](\mathbf{r}_2)\,\mathrm{d}\mathbf{r_2}+\int_{\mathscr{D}}\frac{\delta\mathscr{G}}{\delta q(\mathbf{r}_2)}\left[q\right]\frac{\delta\mathscr{F}}{\delta q(\mathbf{r})}\left[q\right](\mathbf{r}_2)\,\mathrm{d}\mathbf{r_2}=0. \quad (53)$$

If we apply this formula to the critical point q_c we conclude that

$$\int_{\mathscr{D}}\frac{\delta^2\mathscr{G}}{\delta q(\mathbf{r}_2)\delta q(\mathbf{r})}\left[q_c\right]\mathscr{F}\left[q_c\right](\mathbf{r}_2)\mathrm{d}\mathbf{r_2}=0.$$

Using that $\mathscr{G}$ is non degenerate we conclude that for all $\mathbf{r}$

$$\mathscr{F}\left[q_c\right](\mathbf{r})=0$$

and thus q_c is a steady state of the deterministic dynamics.

The remark that critical points of conserved quantity are steady states also extends to the stability properties. Any stable and non degenerate minima or maxima of the conserved quantity is a stable fixed point of the deterministic dynamics (again, think to the energy or angular momentum in mechanics). Those remarks are probably about as old as mechanics. For field problems like ours, the issue may be more subtle. Indeed, one should then be careful of the norm inequivalence (an infinite number of small scales can do a lot). One can see for instance the Arnold stability theorems for the 2D Euler equations [2], or their generalization to many fluid mechanics problems [36].

Another important point is that, from the relations (36) and (38), it is clear that if q_s is a steady state of the deterministic dynamics, then $I[q_s]$ is a steady state of the reversed dynamics, and vice versa. Also if q_c is a critical point of the potential $\mathscr{G}$, then $I[q_c]$ will be a critical point of $\mathscr{G}_r$. The stability properties (minima, global minima, local minima, number of unstable directions, and so on) of q_c with respect to the minimization of $\mathscr{G}$ will be the stability properties of $I[q_c]$ for the minimization of $\mathscr{G}_r$.

4.2.6 Relaxation dynamics and relaxation paths

We call a relaxation path a solution of the relaxation dynamics

$$\frac{\partial q}{\partial t} = \mathscr{F}[q](\mathbf{r}) - \alpha \int_{\mathscr{D}} C(\mathbf{r},\mathbf{r}') \frac{\delta \mathscr{G}}{\delta q(\mathbf{r}')}[q]\, \mathrm{d}\mathbf{r}'. \tag{54}$$

Lyapunov functional for relaxation equation

For any relaxation trajectory $q(t)$, using that $\mathscr{G}$ is conserved by the inertial dynamics we easily prove that

$$\frac{\mathrm{d}}{\mathrm{d}t}\mathscr{G}[q(t)] = -\alpha \int_{\mathscr{D}} C(\mathbf{r},\mathbf{r}') \frac{\delta \mathscr{G}}{\delta q(\mathbf{r}')} \frac{\delta \mathscr{G}}{\delta q(\mathbf{r})} \mathrm{d}\mathbf{r}\mathrm{d}\mathbf{r}' \leq 0,$$

where we have used the positivity of C for establishing the inequality. Then we conclude that $\mathscr{G}$ is a Lyapunov functional for the relaxation dynamics.

From this remark, we conclude that any minima of the potential is stable for the relaxation dynamics.

4.2.7 Action minima, relaxation paths of the dual dynamics, and instantons

We consider action minima, for instance with fixed boundary conditions

$$A(q_0,q_T,T) = \min_{\{q\,|q(0)=q_0 \text{ and } q(T)=q_T\}} \mathscr{A}[q,T].$$

This variational problem is essential for many problems. For instance it describes the most probable path to go from q_0 to q_T. Moreover, as will be discussed in the next section, it will be useful in order to describe large deviation results.

From the definition of the action (42-44), as C is positive, it is clear that

$$A(q_0,q_T,T) \geq 0.$$

Using the action duality relation (49), we also conclude that

$$A(T) \geq 2\{\mathscr{G}[q_T] - \mathscr{G}[q_0]\}. \tag{55}$$

It is clear from the definition of the relaxation paths (54) and from the definition of the action (42-44) that a relaxation path has zero action. This should be clear physically, as no noise is needed for the system to follow such a path and that for a centered Gaussian field (the noise), zero is the most probable field. Then if there exists a relaxation path between q_0 and q_T during time T ($q(t)$ such that $q(0) = q_0$ and $q(T) = q_T$), we conclude that

$$A(q_0,q_T,T) = 0.$$

Similarly, using the duality relation (49), we conclude that if there exists a relaxation path for the reversed dynamics between $I(q_T)$ and $I(q_0)$, we conclude that

$$A(q_0,q_T,T) = 2\{\mathscr{G}[q_T] - \mathscr{G}[q_0]\}.$$

This is an essential remark. Indeed, the reversed dynamics has properties very similar to the initial dynamics (it has the same fixed points, the same attractors, the same saddles up to the application of the involution I), but in the argument above, we see that the final and end-points of the relaxation paths have been exchanged from q_0 and q_T respectively to $I(q_T)$ and $I(q_0)$ respectively. This will be especially useful when the starting point is one of the local minima of the potential $\mathscr{G}$.

We now consider the case when q_0 is a local minimum of $\mathscr{G}$. Then as it is also an attractor of the relaxation dynamics, no non-trivial relaxation path will start at q_0. But for all q_T inside the basin of attraction of q_0 for the relaxation dynamics, there exists a relaxation path from q_T to q_0. Generically, this path will have an infinite length $T = \infty$ (for instance if there is an exponential relaxation). Then there is also a relaxation path for the dual dynamics from $I[q_T]$ to $I[q_0]$.

We thus can conclude that for all q_T in the basin of attraction of an local minima of q_0 for the relaxation dynamics, then

$$A(q_0,q_T,\infty) = 2\{\mathscr{G}[q_T] - \mathscr{G}[q_0]\}.$$

In many problems, for instance when one looks at the stationary distribution, it is important to solve the variational problem

$$A_\infty(q_0,q_T) = \inf_{T\geq 0} \inf_{\left\{ q \,|q(0)=q_0 \text{ and } q(T)=q_T \right\}} \mathscr{A}[q,T].$$

From the last result and the inequality (55), we immediately conclude that for all q_T in the basin of attraction of an local minima of q_0

$$A_\infty(q_0,q_T) = 2\left\{\mathscr{G}[q_T] - \mathscr{G}[q_0]\right\}.$$

If q_T is in basin of attraction of $q_1 \neq 0$, then because there exist a relaxation path from q_T to q_0, we can conclude that

$$A_\infty(q_0,q_T) = A(q_0,q_T,\infty) = A_\infty(q_0,q_1).$$

Moreover, it is easily understood that the action minima will correspond to the relaxation trajectory in the dual dynamics from the lowest saddle $q_s(q_0,q_1)$ that belongs to the closure of the basin of attractions of both q_0 and q_1. Hence

$$A_\infty(q_0,q_T) = A_\infty(q_0,q_1) = 2\left\{\mathscr{G}[q_s(q_0,q_1)] - \mathscr{G}[q_0]\right\}.$$

We thus conclude that the minimizers of the action between local minima of the potential and saddles, during an infinite time, are essential. Those trajectories are called instantons. As it is clear from the previous discussion, instantons are the reversed of relaxation paths for the dual dynamics. Instantons need an infinite time to leave the attractor and an infinite time to converge to the saddle. More explicitly, if $\{q_r(t)\}_{-\infty\leq t\leq\infty}$ is a relaxation path for the reversed dynamics between a saddle $I[q_s]$ and the attractor $I[q_0]$, then the instanton between q_0 and q_s is $\{I[q_r(-t)]\}_{-\infty\leq t\leq\infty}$.

4.2.8 Euler-Langrange equations and Hamiltonian formalism

In this section, we write the Euler-Lagrange equations for the minimization of the action. As it will be more simple, we will use Hamilton formalism in order to do so.

We start from the Lagrangian (42)

$$\mathscr{L}\left[q,\frac{\partial q}{\partial t}\right] = \frac{1}{2\alpha}\int_{\mathscr{D}}\int_{\mathscr{D}}\left(\frac{\partial q}{\partial t} - \mathscr{F}[q](\mathbf{r}) + \alpha\int_{\mathscr{D}} C(\mathbf{r},\mathbf{r}_1)\frac{\delta\mathscr{G}}{\delta q(\mathbf{r}_1)}[q]\,\mathrm{d}\mathbf{r}_1\right)\times \tag{56}$$

$$C^{-1}(\mathbf{r},\mathbf{r}')\left(\frac{\partial q}{\partial t} - \mathscr{F}[q](\mathbf{r}') + \alpha\int_{\mathscr{D}} C(\mathbf{r}',\mathbf{r}_2)\frac{\delta\mathscr{G}}{\delta q(\mathbf{r}_2)}[q]\,\mathrm{d}\mathbf{r}_2\right)\mathrm{d}\mathbf{r}\mathrm{d}\mathbf{r}', \tag{57}$$

and denote $p(\mathbf{r},t)$ the momentum

$$p(\mathbf{r}) \equiv \frac{\delta\mathscr{L}[q,\dot{q}]}{\delta\dot{q}(\mathbf{r})} = \frac{1}{\alpha}\int_{\mathscr{D}} C^{-1}(\mathbf{r},\mathbf{r}')\left(\frac{\partial q}{\partial t}(\mathbf{r}') - \mathscr{F}[q](\mathbf{r}') + \alpha\int_{\mathscr{D}} C(\mathbf{r}',\mathbf{r}_2)\frac{\delta\mathscr{G}}{\delta q(\mathbf{r}_2)}\mathrm{d}\mathbf{r}_2\right)\mathrm{d}\mathbf{r}',$$

where we have used the symmetry of C^{-1}. We note that

$$\frac{\partial q}{\partial t} - \mathscr{F}[q](\mathbf{r}) + \alpha \int_{\mathscr{D}} C(\mathbf{r},\mathbf{r}_2) \frac{\delta \mathscr{G}}{\delta q(\mathbf{r}_2)} \mathrm{d}\mathbf{r}_2 = \alpha \int_{\mathscr{D}} C(\mathbf{r},\mathbf{r}') p(\mathbf{r}') \mathrm{d}\mathbf{r}'. \tag{58}$$

4.2.9 Hamiltonian

The Hamiltonian associated to the action minimization is defined as

$$\mathscr{H}[p,q] = \int_{\mathscr{D}} \left[p(\mathbf{r}) \frac{\partial q}{\partial t}(\mathbf{r}) - \frac{1}{2\alpha} \left(\frac{\partial q}{\partial t} - \mathscr{F}[q](\mathbf{r}) + \alpha \int_{\mathscr{D}} C(\mathbf{r},\mathbf{r}_1) \frac{\delta \mathscr{G}}{\delta q(\mathbf{r}_1)} \mathrm{d}\mathbf{r}_1 \right) \times \right.$$
$$\left. \int_{\mathscr{D}} C^{-1}(\mathbf{r},\mathbf{r}') \left(\frac{\partial q}{\partial t} - \mathscr{F}[q](\mathbf{r}') + \alpha \int_{\mathscr{D}} C(\mathbf{r}',\mathbf{r}_2) \frac{\delta \mathscr{G}}{\delta q(\mathbf{r}_2)} \mathrm{d}\mathbf{r}_2 \right) \mathrm{d}\mathbf{r}' \right] \mathrm{d}\mathbf{r}$$

which leads, using (58), to

$$\mathscr{H}[p,q] = \frac{\alpha}{2} \int_{\mathscr{D}} \int_{\mathscr{D}} p(\mathbf{r}) C(\mathbf{r},\mathbf{r}') p(\mathbf{r}') \mathrm{d}\mathbf{r} \mathrm{d}\mathbf{r}' - \tag{59}$$

$$\int_{\mathscr{D}} p(\mathbf{r}) \left(-\mathscr{F}[q](\mathbf{r}) + \alpha \int_{\mathscr{D}} C(\mathbf{r},\mathbf{r}_1) \frac{\delta \mathscr{G}}{\delta q(\mathbf{r}_1)} \mathrm{d}\mathbf{r}_1 \right) \mathrm{d}\mathbf{r}. \tag{60}$$

4.2.10 Euler-Lagrange equations

The Euler-Langrange equations for the action minimization or for the instanton dynamics are given by

$$\frac{\partial q}{\partial t} = \frac{\delta \mathscr{H}}{\delta p} \text{ and } \frac{\partial p}{\partial t} = -\frac{\delta \mathscr{H}}{\delta q}.$$

It leads to

$$\frac{\partial q}{\partial t}(\mathbf{r}) = \mathscr{F}[q](\mathbf{r}) - \alpha \int_{\mathscr{D}} C(\mathbf{r},\mathbf{r}') \frac{\delta \mathscr{G}}{\delta q(\mathbf{r}')} \mathrm{d}\mathbf{r}' + \alpha \int_{\mathscr{D}} C(\mathbf{r},\mathbf{r}') p(\mathbf{r}') \mathrm{d}\mathbf{r}', \tag{61}$$

and

$$\frac{\partial p}{\partial t}(\mathbf{r}) = -\int_{\mathscr{D}} p(\mathbf{r}_1) \left(\frac{\delta \mathscr{F}}{\delta q(\mathbf{r})}[q](\mathbf{r}_1) - \alpha \int_{\mathscr{D}} C(\mathbf{r}_1,\mathbf{r}_2) \frac{\delta \mathscr{G}}{\delta q(\mathbf{r}_1) \delta q(\mathbf{r})} \mathrm{d}\mathbf{r}_2 \right) \mathrm{d}\mathbf{r}_1 \tag{62}$$

Consistency check

It is easily checked that any relaxation path

$$\frac{\partial q}{\partial t} = \mathscr{F}[q](\mathbf{r}) - \alpha \int_{\mathscr{D}} C(\mathbf{r},\mathbf{r}') \frac{\delta \mathscr{G}}{\delta q(\mathbf{r}')} \mathrm{d}\mathbf{r}'$$

with $p = 0$, is a solution to the instanton equations (61-62).

Moreover any reversed relaxation path of the dual dynamics, solving $q(t) = I[q_r(-t)]$ with

$$\frac{\partial q_r}{\partial t} = \mathscr{F}_r[q_r](\mathbf{r}) - \alpha \int_{\mathscr{D}} C_r(\mathbf{r},\mathbf{r}') \frac{\delta \mathscr{G}_r}{\delta q(\mathbf{r}')}[q_r]\,\mathrm{d}\mathbf{r}'$$

or equivalently

$$\frac{\partial q}{\partial t} = \mathscr{F}[q](\mathbf{r}) + \alpha \int_{\mathscr{D}} C(\mathbf{r},\mathbf{r}') \frac{\delta \mathscr{G}}{\delta q(\mathbf{r}')}[q]\,\mathrm{d}\mathbf{r}' \tag{63}$$

together with

$$p(\mathbf{r}) = 2\frac{\delta \mathscr{G}}{\delta q(\mathbf{r})}[q] \tag{64}$$

should also be solution to the instanton equations (61-62). We check this. From this last expression, we have

$$\frac{\partial p}{\partial t}(\mathbf{r}) = 2\int_{\mathscr{D}} \frac{\delta^2 \mathscr{G}}{\delta q(\mathbf{r})\delta q(\mathbf{r}_1)}[q] \frac{\partial q}{\partial t}(\mathbf{r}_1)\,\mathrm{d}\mathbf{r}_1$$

Then using (63)

$$\frac{\partial p}{\partial t}(\mathbf{r}) = 2\int_{\mathscr{D}} \frac{\delta^2 \mathscr{G}}{\delta q(\mathbf{r})\delta q(\mathbf{r}_1)}[q] \left(\mathscr{F}[q](\mathbf{r}_1) + \alpha \int_{\mathscr{D}} C(\mathbf{r}_1,\mathbf{r}') \frac{\delta \mathscr{G}}{\delta q(\mathbf{r}')}[q]\,\mathrm{d}\mathbf{r}' \right) \mathrm{d}\mathbf{r}_1 \mathrm{d}\mathbf{r}_2$$

which using (64) and (53) gives (62) as expected.

4.2.11 Hamiltonian value for instantons

We prove that instanton, or any action minimizer that converges for $t \to \infty$ to one fixed point (let say q_0 for t going to ∞) has a zero value for the Hamiltonian. Then, for $t \to \infty$, we have

$$\frac{\partial q}{\partial t} \overset{t\to\infty}{\to} 0.$$

Moreover as q_0 is an attractor

$$\mathscr{F}[q_0] = 0$$

and

$$\frac{\delta \mathscr{G}}{\delta q(\mathbf{r})}[q_0] = 0.$$

Then from equation (61), using that C is invertible, we get

$$p \overset{t\to\infty}{\to} 0.$$

Using all these relations we conclude that along an instanton the value of the Hamiltonian (59) is

$$\mathscr{H} = 0.$$

4.3 Instantons for the Langevin dynamics of the 2D-Euler and Quasi-Geostrophic equilibrium dynamics

We consider the Langevin dynamics associated to the quasigeostrophic equations in a periodic domain $\mathscr{D} = [0, 2l_x\pi) \times [0, 2\pi)$ with aspect ratio l_x:

$$\frac{\partial q}{\partial t} + \mathbf{v}[q-h]\cdot\nabla q = -\alpha \int_{\mathscr{D}} C(\mathbf{r},\mathbf{r}') \frac{\delta \mathscr{G}}{\delta q(\mathbf{r}')} \mathrm{d}\mathbf{r}' + \sqrt{2\alpha\gamma}\eta, \tag{65}$$

$$\mathbf{v} = \mathbf{e}_z \times \nabla\psi, \quad q = \omega + h(y) \tag{66}$$

and potential $\mathscr{G}$. We consider G the green function of the Laplacian ($G = \Delta^{-1}$), such that the equations between the potential vorticity, stream function and velocity are inverted as

$$\psi(\mathbf{r}) = \int_{\mathscr{D}} G\left(\mathbf{r},\mathbf{r}'\right)(q-h)(\mathbf{r}')\mathrm{d}\mathbf{r}',$$

and

$$\mathbf{v}[\omega](\mathbf{r}) = \int_{\mathscr{D}} \mathbf{e}_z \times \nabla_{\mathbf{r}_1} G\left(\mathbf{r},\mathbf{r}'\right)\omega(\mathbf{r}')\mathrm{d}\mathbf{r}'. \tag{67}$$

($\mathbf{v}[\omega]$ is the operator that allows to compute the velocity from the vorticity). When $h = 0$, this dynamics is the 2D-Euler equilibrium dynamics.

4.3.1 Reversed dynamics and detailed balance

Then the formalism of section 4 applies with $\mathscr{F}[q] = -\mathbf{v}[q-h]\cdot\nabla q$.

For the 2D Euler or quasi-geostrophic equation, the relevant involution corresponding to time reversal is

$$I[q] = -q.$$

Using (36-38) we conclude that

$$\mathscr{F}_r[q] = \mathbf{v}[q+h]\cdot\nabla q,$$

$C_r = C$ and

$$\mathscr{G}_r[q] = \mathscr{G}[-q].$$

From these equation, we see that for the 2D Euler equations ($h = 0$), $\mathscr{F}_r = \mathscr{F}$ and the dynamics is time-reversible (see Eq. 36). The time reversibility condition on $\mathscr{G}$ (see Eq. 41) is that $\mathscr{G}$ be even. We thus have two cases:

1. For the 2D-Euler equations and when $\mathscr{G}$ is even, the Langevin dynamics is time-reversible and we have detailed balance.
2. When either $h \neq 0$ (Quasi-Geostrophic) or $\mathscr{G}$ is not even, then the Langevin dynamics is not time-reversible. It is conjugated to another Langevin dynamics where h has to be replaced by $-h$ and $\mathscr{G}$ by $\mathscr{G}_r[q] = \mathscr{G}[-q]$. Detailed balance is not verified.

4.3.2 Instanton equation

As discussed in section 4, the instantons from one attracting point to a saddle are the reverse of the relaxation paths for the reversed dynamics. From (54) applied to the case $\mathscr{F}_r[q] = \mathbf{v}[q+h]\cdot\nabla q$, and $\mathscr{G}_r[q] = \mathscr{G}[-q]$, we conclude that the equation of those relaxation paths is

$$\frac{\partial q}{\partial t} + \mathbf{v}[q+h]\cdot\nabla q = -\alpha \int_{\mathscr{D}} C(\mathbf{r},\mathbf{r}') \frac{\delta \mathscr{G}}{\delta q(\mathbf{r}')}[-q]\,\mathrm{d}\mathbf{r}'. \tag{68}$$

We also write explicitly the Euler-Lagrange equation in the qausi-geostrophic case. Writing (61-62) in the case $\mathscr{F}[q] = -\mathbf{v}[q-h]\cdot\nabla q$, and using

$$\frac{\delta \mathbf{v}}{\delta q(\mathbf{r})}[q-h](\mathbf{r}_1) = \mathbf{e}_z \times \nabla_{\mathbf{r}_1} G(\mathbf{r}_1,\mathbf{r}). \tag{69}$$

we obtain

$$\frac{\partial q}{\partial t}(\mathbf{r}) + \mathbf{v}[q-h]\cdot\nabla q = -\alpha \int_{\mathscr{D}} C(\mathbf{r},\mathbf{r}') \frac{\delta \mathscr{G}}{\delta q(\mathbf{r}')}\mathrm{d}\mathbf{r}' + \alpha \int_{\mathscr{D}} C(\mathbf{r},\mathbf{r}') p(\mathbf{r}')\mathrm{d}\mathbf{r}', \tag{70}$$

and

$$\frac{\partial p}{\partial t}(\mathbf{r}) + \mathbf{v}[q-h]\cdot\nabla p = \alpha \int_{\mathscr{D}} p(\mathbf{r}_1) \int_{\mathscr{D}} C(\mathbf{r}_1,\mathbf{r}_2) \frac{\delta^2 \mathscr{G}}{\delta q(\mathbf{r}_1)\delta q(\mathbf{r})}\mathrm{d}\mathbf{r}_2\mathrm{d}\mathbf{r}_1 \tag{71}$$

$$+ \int_{\mathscr{D}} p(\mathbf{r}_1)\mathbf{e}_z \times \nabla_{\mathbf{r}_1} G(\mathbf{r}_1,\mathbf{r}).\nabla q\,\mathrm{d}\mathbf{r}_1 \tag{72}$$

or equivalently

$$\frac{\partial p}{\partial t}(\mathbf{r}) + \mathbf{v}[q-h]\cdot\nabla p = \alpha \int_{\mathscr{D}} p(\mathbf{r}_1) \int_{\mathscr{D}} C(\mathbf{r}_1,\mathbf{r}_2) \frac{\delta^2 \mathscr{G}}{\delta q(\mathbf{r}_1)\delta q(\mathbf{r})}\mathrm{d}\mathbf{r}_2\mathrm{d}\mathbf{r}_1 \tag{73}$$

$$+ \int_{\mathscr{D}} G(\mathbf{r}_1,\mathbf{r})\,(\nabla q \times \nabla p)(\mathbf{r}_1).\mathbf{e}_z\,\mathrm{d}\mathbf{r}_1. \tag{74}$$

4.3.3 Phase transition between zonal flows in a barotropic Quasi-Geostrophic model with topography

In order to fully specify the quasi-geostrophic Langevin dynamics (65) we need to specify the topography function and a choice of the potential $\mathscr{G}$. Given the infinite number of conserved quantities for the quasi-geostrophic dynamics, there are many possible choices. We want to describe the phenomenology of phase transitions and instanton theory in a situation of first order transition. We will illustrate such a phenomenology through two examples.

For the first example, we choose a topography $h(\mathbf{r}) = H\cos(2y)$, such that

$$q = \Delta\psi + H\cos(2y),$$

and we consider the potential

$$\mathscr{G} = \mathscr{C} + \beta\mathscr{E}, \tag{75}$$

with energy (4), β is the inverse temperature, and where $\mathscr{C}$ is the Casimir functional

$$\mathscr{C} = \int_{\mathscr{D}} \mathrm{d}\mathbf{r}\left[\frac{q^2}{2} - a_4\frac{q^4}{4} + a_6\frac{q^6}{6}\right], \tag{76}$$

where we assume $a_6 > 0$.

4.3.4 Zonal phase transitions

We first look at the structure of the minima of the potential $\mathscr{G}$ (75), and their bifurcations when the parameters ε and a_4 are changed, where ε is defined by

$$\beta = -1 + \varepsilon.$$

At low positive temperature ($\beta \to +\infty$) we expect to see energy minima, which correspond to $\psi = 0$ and $q = H\cos(2y)$. As the energy is convex, for positive β and small enough a_4, both $\mathscr{C}$ and $\beta\mathscr{E}$ will be convex, then we expect that $\mathscr{G}$ has a unique global minimum and no local minima. For large enough β, this equilibrium state will be dominated by the topographic effect. For small negative β, the change of convexity of $\beta\mathscr{E}$ from convex to concave will not change this picture. However for smaller β (more negative and higher absolute value), we expect a phase transition to occur as the potential $\mathscr{G}$ will become locally concave. If $a_4 > 0$ with sufficiently large values this will be a first order phase transition. If $a_4 < 0$ with sufficiently large values, this will be a second order phase transition.

For $H = 0$, a bifurcation occurs for $\beta = -1$ ($\varepsilon = 0$) and $a_4 = 0$, as can be easily checked (see for instance [24]). For $H = 0$, this bifurcation is due to the vanishing of the Hessian at $\beta = -1$ ($\varepsilon = 0$) and $a_4 = 0$. As discussed in many paper [22, 69, 13, 24], for quadratic Casimir functional $\mathscr{C}_2 = \int_{\mathscr{D}} \mathrm{d}\mathbf{r}\,\frac{q^2}{2}$, the first bifurcation involves the eigenfunction of $-\Delta$ with the lowest eigenvalue. If we assume that the aspect ratio

l_x (defined just before equation (65)) verifies $l_x < 1$, then this smallest eigenvalue is the one corresponding to the zonal mode proportional to $\cos(y)$. As we are interested by transition between zonal states, we assume in all this section that $l_x < 1$.

For non zero but sufficiently small H there will still be a bifurcation for ε and a_4 close to zero. We study this bifurcation in the following. The null space of the Hessian is spanned by eigenfunctions $\cos(y)$ and $\sin(y)$. As a consequence, for small enough ε, a_4 and H we expect the bifurcation to be described by a normal form involving only the projection of the field q on this null space. Hence, we decompose the fields on a contribution over this null space and its orthogonal complement:

$$\psi = A\cos(y) + B\sin(y) + \psi' \tag{77}$$

with $\int_{\mathscr{D}} \mathrm{d}\mathbf{r}\, \mathrm{e}^{iy} \psi'(\mathbf{r}) = 0$. Then

$$q = -A\cos(y) - B\sin(y) + q', \tag{78}$$

with $\int_{\mathscr{D}} \mathrm{d}\mathbf{r}\, \mathrm{e}^{iy} q'(\mathbf{r}) = 0$. The fact that the bifurcation can be described by a normal form over the null space of the Hessian can be expected on a general ground. It can actually be justified by using Lyapunov–Schmidt reduction, as done and explained in [24] for a number of examples for the 2D-Euler and quasi-geostrophic equations. Then all other degrees of freedoms describing the minima q_c of $\mathscr{G}$ are slaved to A and B, in the sense that they can be simply expressed as functions of A and B. Even if the following example is not treated in the paper [24], and if it could clearly be done without much difficulty, we do not describe the detail of the Lyapunov–Schmidt reduction here, for simplicity. We rather propose a more heuristic discussion.

We will treat the problem perturbatively by assuming that $\varepsilon \ll 1$, $\varepsilon a_6 \ll a_4^2$, and $a_4 H^2 \ll \varepsilon$ (we note that it implies that $a_6 H^4 \ll \varepsilon$). We make these assumptions in order to get an explicit description of the phase transitions, however it is important to understand that the theory that predicts the transitions rates and the instantons does not depend on those asumptions and that the same phenomenology will remain valid beyond the perturbative regime. Then we will assume that ψ' and q' are first order corrections in all the three perturbation parameters. We then rewrite the potential $\mathscr{G}$, taking into account only the leading order contributions. From (4), (76) and (77-78), after straightforward computations we have

$$\mathscr{E} = \pi^2 l_x \left[A^2 + B^2\right] + \frac{1}{2}\int_{\mathscr{D}} \mathrm{d}\mathbf{r}\, \left[H\cos(2y) - q'\right] \psi'$$

and

$$\mathscr{G} = \pi^2 l_x \mathscr{G}_0(A,B) + \mathscr{G}_1(A,B)\left[q'\right] + \text{lower order terms}$$

with

$$\mathscr{G}_0(A,B) = \varepsilon\left[A^2 + B^2\right] - \frac{3a_4}{8}\left[A^2 + B^2\right]^2 + \frac{5a_6}{24}\left[A^2 + B^2\right]^3 + \mathrm{O}(\varepsilon a_4),$$

and

$$\mathscr{G}_1(A,B)[q'] = \tfrac{1}{2}(\varepsilon-1)\int_{\mathscr{D}}[H\cos(2y)-q']\,\psi'\,\mathrm{d}\mathbf{r} \tag{79}$$
$$+\int_{\mathscr{D}}\left\{\tfrac{q'^2}{2}\left[1-3a_4\left[A\cos(y)+B\sin(y)\right]^2+5a_6\left[A\cos(y)+B\sin(y)\right]^4\right]\right\}\mathrm{d}\mathbf{r}$$

We assume that $a_4A^2 \ll \varepsilon$, $a_6A^4 \ll \varepsilon$ and $\varepsilon \ll 1$. Then the leading order terms are obtained from the minimization of the first integral and

$$\psi' = \left[\frac{H}{3}\cos(2y)\right]\left[1+\mathrm{O}(\varepsilon)+\mathrm{O}\left(a_4A^2\right)+\mathrm{O}\left(a_6A^4\right)\right],$$

or equivalently

$$q' = -\frac{H}{3}\cos(2y)\left[1+\mathrm{O}(\varepsilon)+\mathrm{O}\left(a_4A^2\right)+\mathrm{O}\left(a_6A^4\right)\right].$$

We use this expression in order to compute the leading order contributions to $G_1(A,B) = \min_{\{q'\}}\mathscr{G}_1(A,B)[q']$. After lengthy but straightforward computations, we get at leading order

$$G_1 = \min_q \mathscr{G}_1 = -\frac{H^2}{3} - \frac{\pi^2 l_x a_4 H^2}{6}\left[A^2+B^2\right] + \frac{5\pi^2 l_x a_6 H^2}{144}\left(5\left[A^2+B^2\right]^2+2\left[A^2-B^2\right]^2\right),$$

and then

$$\min_q \mathscr{G} = \min_{(A,B)} \pi^2 l_x G(A,B) \tag{80}$$

with G given at leading order by

$$G(A,B) = -\tfrac{H^2}{3}+\left(\varepsilon-\tfrac{a_4H^2}{6}+\tfrac{5a_6H^4}{216}\right)\left[A^2+B^2\right] \tag{81}$$
$$+\left(-\tfrac{3a_4}{8}+\tfrac{25a_6H^2}{144}\right)\left[A^2+B^2\right]^2+\left(\tfrac{5a_6}{24}\right)\left[A^2+B^2\right]^3+\left(\tfrac{5a_6H^2}{72}\right)\left[A^2-B^2\right]^2.$$

$G(A,B)$ is the normal form that describes the phase transition for $a_4A^2 \ll 1$, and $a_6A^4 \ll 1$ and $\varepsilon \ll 1$.

The fact that G is a normal form for small enough a_4, a_6, and H implies that the gradient of $\mathscr{G}$ in direction transverse to $q = A\cos(y)+B\sin(y)$ are much steeper than the gradient of G. A more complete derivation could easily be performed, for instance along the line discussed in [24].

The term proportional to $\left(A^2-B^2\right)^2$ breaks the symmetry between A and B. Its minimization imposes $A^2 = B^2$. Then either $A = B$, or $A = -B$. If we take into account that minimizing with respect to A^2+B^2 will only give the absolute value of A, we conclude that we will have 4 equivalent solutions

$$q_i = -\frac{H}{3}\cos(2y) + \sqrt{2}\,|A|\,(\varepsilon,a_4,a_6)\cos(y+\phi_i),$$

with ϕ_i taking one of the four value $\left\{-\frac{3\pi}{4},-\frac{\pi}{4},\frac{\pi}{4},\frac{3\pi}{4}\right\}$, and $|A|$ minimizing

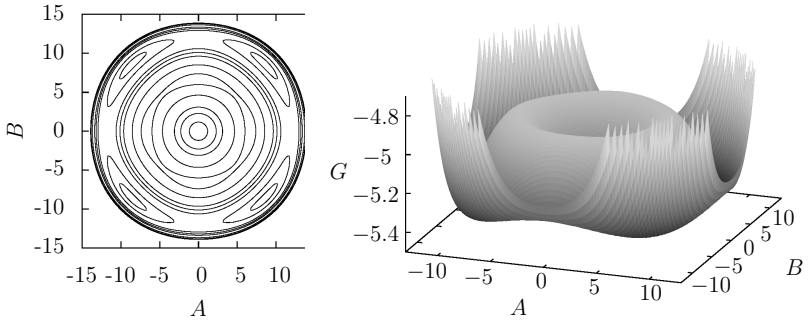

Fig. 10 The reduced potential surface $G(A,B)$ (see Eq. (81)) for parameter values $\varepsilon > 0$ and $a_4 > 0$. For those parameter, G has four global minima with $|A| = |B|$. This structure with four attractors is due to a breaking of the symmetry imposed by the topography $h(y) = H\cos(2y)$ (see section 4.3.4). For $\varepsilon < 0$, the minima of G have the symmetries of h (the potential vorticity profile have a reflexion symmetry with respect to both $y = 0$ or $y = \pi$ and an antireflexion symmetry with respect to both $y = \pi/2$ and $y = 3\pi/2$). For $\varepsilon > 0$ this symmetry is broken leading to four different attractors. Parameters for the reduced potential are: $\varepsilon = 1.6\times10^{-2}$, $H = 4$, $a_4 = 6\times10^{-4}$, $a_6 = 3.6\times10^{-6}$.

$$\tilde{G}(|A|) = -\frac{H^2}{3} + 2\left(\varepsilon - \frac{a_4H^2}{6} + \frac{5a_6H^4}{216}\right)|A|^2 + 4\left(\frac{3a_4}{8} + \frac{25a_6H^2}{144}\right)|A|^4 + \frac{5a_6}{3}|A|^6 . \tag{82}$$

The reduced potential G is plotted on figure 10 in the case $\varepsilon > 0$ and $a_4 > 0$. This structure with four attractors is due to a breaking of the symmetry imposed by the topography $h(y) = H\cos(2y)$. For $\varepsilon < 0$, the minima of G have the symmetries of h (the potential vorticity profile have a reflexion symmetry with respect to both $y = 0$ or $y = \pi$ and an antireflection symmetry with respect to both $y = \pi/2$ and $y = 3\pi/2$). For $\varepsilon > 0$ this symmetry is broken leading to four different attractors. The potential vorticities of one of the attractors and of one of the saddle points are shown in figure 11.

Looking at the reduced potential $\tilde{G}$ (equation 82), we recognize the structure of a tricritical point: a point at which a first order transition line is changed to a second order transition line. Figure 12 shows a phase diagram for the normal form for a tricritical point. The reduced potential $\tilde{G}$ (equation 82) corresponds to this normal form with $a = \frac{2}{5a_6}\left(\varepsilon - \frac{a_4H^2}{6} + \frac{5a_6H^4}{216}\right)$ and $b = \frac{8}{5a_6}\left(\frac{3a_4}{8} + \frac{25a_6H^2}{144}\right)$.

From this last equation, we conclude that: for $a_4 < \frac{25a_6H^2}{54}$ ($a_4 < 0$ at leading order), we have a continuous phase transition for $\varepsilon = \frac{35a_6H^4}{648}$ (zero at leading order). For $a_4 = \frac{25a_6H^2}{54}$ ($a_4 = 0$ at leading order), we have a tricritical point. The transition is between a state which is given at leading order by

$$q = -\frac{H}{3}\cos(2y)$$

and one of the four states given by

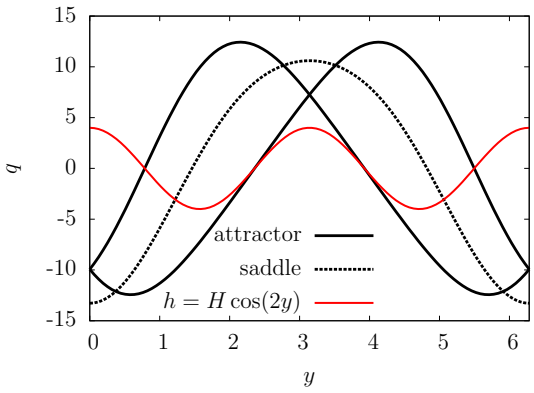

Fig. 11 The plot shows the topography ($h(y) = H\cos(2y)$, symmetric red curve) and two attractors of the potential vorticity q (black solid lines) corresponding to two of the minima of the effective potential G (see equation 81, and figure 10) for parameter values $\varepsilon > 0$ and $a_4 > 0$. Additionally, we present one of the saddles between the two attractors of the effect potential G.

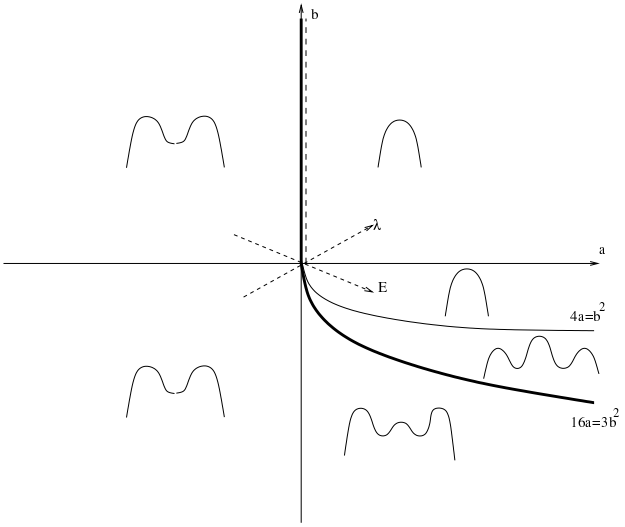

Fig. 12 This figure shows the phase diagram for a tricritical point corresponding to the maximization of the normal form $s(m) = -m^6 - \frac{3b}{2}m^4 - 3am^2$ (from [7]). The inset shows the qualitative shape of the potential s when the parameters a and b are changed. The bold line is a line of first order phase, or discontinuous phase transition. The bold-dashed line is a second order phase transition line. At the tricritical point ($a = b = 0$), the first order phase transition changes to a second order phase transition.

$$q_i = -\frac{H}{3}\cos(2y) + \sqrt{2}\,|A|\,(\varepsilon, a_4, a_6)\cos(y+\phi_i), \tag{83}$$

where $\phi_i \in \left\{-\frac{3\pi}{4}, -\frac{\pi}{4}, \frac{\pi}{4}, \frac{3\pi}{4}\right\}$, and $|A|\,(\varepsilon, a_4, a_6)$ is the non-zero minimizer of (82). For $a_4 > 0$ and ε close to zero, we have coexistence between these two states, and thus the transition when ε is increased is a first order transition. For $a_4 < 0$ and ε close to zero, the transition when ε is increased is a second order transition (continuous transition).

4.3.5 Instantons for the topography phase transition

We know describe and compute the instantons corresponding to the phase transition between zonal flows, discussed in the previous section. In section 4 we have derived the general theory of Langevin dynamics for field problems with potential $\mathscr{G}$. We have concluded in section 4.3 that instantons are the time reversed of relaxation paths for the reversed dynamics. The equation for the relaxation paths for the reversed dynamics of the Quasi-Geostrophic dynamics have been derived in section 4.3 (equation (68)).

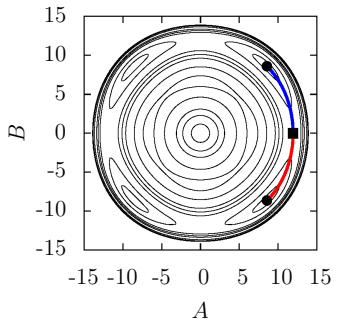

Fig. 13 The reduced potential surface $G(A,B)$ (same as figure 10) with superimposed the path followed by both instantons (fluctuation path from one attractor to a saddle) and relaxation paths (red line). For this case, the fluctuation and relexation paths are actually the reversed of each other, so that the red line shows an instanton from one attractor followed by a relaxation to another attractor, or vice versa.

The general theory and equation (68) show that for the Quasi-Geostrophic dynamics, the reversed dynamics is the Quasi-Geostrophic dynamics where h has been replaced by $-h$ and $\mathscr{G}$ by $\mathscr{G}_r$, with $\mathscr{G}_r[q] = \mathscr{G}[-q]$. In the example we discussed now, $\mathscr{G}$ is even (see equation (76)) such that $\mathscr{G}_r = \mathscr{G}$. We remark also that over the set of zonal flows $\mathbf{v} = U(y)\mathbf{e}_x$, the non-linear term of the Quasi-Geostrophic equation identically vanish: $\mathbf{v}[q+h].\nabla q = 0$. As a consequence, when the instanton remains a zonal flow, the fact that h has to be replaced by $-h$ has no consequence. Let us now argue that the instanton is actually generically a zonal flow.

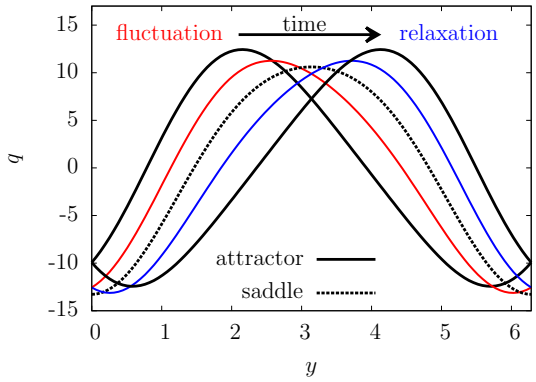

Fig. 14 The potential vorticity q versus y for two of the attractors (blue and red curves), the saddle passed by the instanton (light green curve) and two intermediate profiles along the instanton dynamics or relaxation dynamics (purple or dark green curves).

We assume for simplicity that the stochastic forces are homogeneous (invariant by translation in both directions). Then $C(\mathbf{r},\mathbf{r}') = C(\mathbf{r}-\mathbf{r}') = C_z(y-y') + C_m(y-y', x-x')$ where

$$C_z(y) = \frac{1}{2\pi l_x}\int_0^{2\pi l_x} C(x,y)\mathrm{d}x$$

is the zonal part of the correlation function, and $C_m = C - C_z$ the non-zonal part.

As the non-linear term of the Quasi-Geostrophic equation identically vanishes, the relaxation dynamics has a solution among the set of zonal flows. If C_z is non-degenerate (positive definite as a correlation function), then relaxation paths will exist through the gradient dynamics

$$\frac{\partial q}{\partial t} = -2\pi\alpha l_x \int_0^{2\pi} \mathrm{d}y C_z(y-y')\frac{\delta \mathscr{G}}{\delta q(y')}\mathrm{d}y', \tag{84}$$

where $q = q(y)$ is the zonal potential vorticity field.

Moreover, as argued in section 4.3.4, the fact that G (10) is a normal form for small enough a_4, a_6, and H, implies that the gradient of $\mathscr{G}$ in directions transverse to $q = A\cos(y) + B\cos(y)$ are much steeper than the gradient of G. As a consequence, at leading order the relaxation paths will be given by the relaxation paths for the effective two-degrees of freedom G. Then, from (80), (81), and (84), we obtain that at leading order the relaxation path is given by (77-78) where the dynamics of A and B is given by

$$\frac{\mathrm{d}A}{\mathrm{d}t} = -c\frac{\partial G}{\partial A} \text{ and } \frac{\mathrm{d}B}{\mathrm{d}t} = -c\frac{\partial G}{\partial B},$$

with $c = -\alpha l_x \int_0^{2\pi} \mathrm{d}y C_z(y')\cos(y')$. We recall that G is given by equation (81).

From this result the relaxation paths are easily computed. Using that fluctuation paths are time reversed of relaxation paths, instanton are also easily computed. One of the resulting relaxation paths and one of the instantons are depicted on figure 13

on the top G in a (A,B) plane. The two attractor involved, together with the saddle point and two intermediate states are shown on figure 14.

4.4 Instantons for non-equilibrium steady states of the 2D Navier-Stokes equations, experiments and related dynamics

In sections 4.1 to 4.3.4 we have discussed situations of bistability close to a first order phase transitions, in Langevin dynamics. Langevin dynamics are equilibrium stochastic dynamics in the sense that the stochastic process is either time reversible, or its time reversal is another Langevin dynamics with a clear physical interpretation, as explained in sections 4.1 and 4.2. This situation occurs often in physics for systems in contact with a thermal bath. However the conditions for such Langevin dynamics are usually not met for real turbulent flows, as most of the times the forcing mechanisms, usually at large scale, are of a completely different nature from the dissipative mechanisms, usually transfering energy to molecular degrees of freedom through viscous effects or other mesoscopic transport phenomena.

The main objective of this section is to relax the equilibrium Langevin hypothesis and to present applications of large deviation theory to genuine non-equilibrium phase transitions. This part of the theory of two-dimensional and geophysical flows is beeing developped currently and a complete picture does not exist yet. However several aspects have been understood recently. The aim of this section is to briefly present those aspects and to refer to more technical papers for a detailed discussion. We begin with the two-dimensional stochastic Navier-Stokes equations in section 4.4.1 where we discuss the numerical computation of non-equilibrium instantons, the existence or not of large deviations, and the large deviation rate. In section 4.4.2 we briefly present experimental studies of non-equilibrium phase-transitions. In section 4.4.3 we discuss non-equilibrium phase transition in systems with long range interactions, which are closely related to the two-dimensional Euler and Navier-Stokes equations and more easily tractable theoretically.

Those three subsection present a mix of theoretical results, modelling, numerical and experimental results. A complete theoretical approach goes through a kinetic theory as discussed in section 5.

4.4.1 Large deviations and minimal action paths for the two-dimensional Navier-Stokes equations

At a phase transition, physical systems undergo drastic qualitative changes. Hence phase transitions play an essential role in the understanding of the macroscopic behavior of any system with a large number of degrees of freedom. In section 3, figure 3.4 on 19 show that the two-dimensional Euler equation on a torus undergo a phase transition from dipoles (one anticyclone and a cyclone) to parallel flows. Based on this observation, similar phase transitions have been searched and observed in nu-

merical simulations of the two-dimensional Navier–Stokes equations [10]. Fig. 4, on page 6, shows bistability and those rare transitions between two attractors. The system has evolved to an apparent non-equilibrium steady state, in which most of the time, the system's dynamics is concentrated around two sets of attractors, namely the vortex dipole and parallel flow. However, at long time intervals, the system sporadically switches between these two large scale attractors. Our aim is to understand this switching behavior with large deviation theory.

A more complete study will be presented in works to be published soon. We only discuss here two simple ideas. We first show that the most probable paths from one attractor to another can be computed numerically. Then we discuss the main theoretical issue: do large deviation exist for this system and what is the large deviation rate.

We start from the two-dimensional Navier-Stokes equations

$$\frac{\partial \omega}{\partial t} + \mathbf{v}[\omega]\cdot\nabla\omega = -\alpha\omega + \nu\Delta\omega + \sqrt{2\alpha}\eta, \tag{85}$$

$$\mathbf{v} = \mathbf{e}_z \times \nabla\psi, \qquad \omega = \Delta\psi, \tag{86}$$

where ω, $\mathbf{v}$ and ψ are respectively the vorticity, the non-divergent velocity, and the streamfunction. This is the same as equation 38 in the case $h = 0$, then $\omega = q$. The curl of the forcing $\eta(\mathbf{x},t)$ is a white in time Gaussian field defined by $\langle \eta(\mathbf{x},t)\eta(\mathbf{x}',t')\rangle = C(\mathbf{x}-\mathbf{x}')\delta(t-t')$, where C is the correlation function of a stochastically homogeneous noise. We stress that in general this is not a Langevin dynamics as defined in section 4.2. Discussion on the qualitative behavior of the turbulent flow generated by these stochastic equations, of the different regimes, of the non-dimensionalization of the equation leading to the scaling of the force with $\sqrt{\alpha}$ are discussed in [16].

The path integral formalism introduced in section 4.1 to 4.3.4 can be used irrespectively of the reversibility of the process. We can thus express transition probabilities in terms of path integrals. Generalizing (42) and (44), on page 30, the Lagrangian $\mathscr{L}$ associated to the two-dimensional Navier–Stokes equations (85) is

$$\mathscr{L}\left[q,\frac{\partial q}{\partial t}\right] = \frac{1}{2\alpha}\int_{\mathscr{D}}\int_{\mathscr{D}}\left(\frac{\partial\omega}{\partial t}(\mathbf{r}) + \mathbf{v}[\omega]\cdot\nabla\omega(\mathbf{r}) + \alpha\omega(\mathbf{r}) - \nu\Delta\omega(\mathbf{r})\right)C^{-1}(\mathbf{r},\mathbf{r}') \tag{87}$$
$$\times\left(\frac{\partial\omega}{\partial t}(\mathbf{r}') + \mathbf{v}[\omega]\cdot\nabla\omega(\mathbf{r}') + \alpha\omega(\mathbf{r}') - \nu\Delta\omega(\mathbf{r}')\right)\mathrm{d}\mathbf{r}\mathrm{d}\mathbf{r}',$$

and the action functional is

$$\mathscr{A}[q,T] = \int_0^T \mathscr{L}\left[q(t),\frac{\partial q}{\partial t}(t)\right]\mathrm{d}t. \tag{88}$$

The transition probability to go from the state q_0 at time 0 to the state q_T at time T, denoted $P[q_T,T;q_0,0]$, can then be expressed as

$$P\left[q_T,T;q_0,0\right]=\int_{\left\{q\,\middle|\,\begin{array}{l}q_{(0)}=q_0\\ q_{(T)}=q_T\end{array}\right\}}\mathscr{D}\left[q\right]\mathrm{e}^{-\frac{\mathscr{A}}{2}}, \tag{89}$$

Numerical computation of the least action path

The minimizer of the action with fixed initial and final state ($q(0)=q_0$ and $q(T)=q_T$) then represents the most probable transition from q_0 to q_T. Without the help of the time reversibility it is much more difficult to have a picture of this transition path.

However the minimization of the action can be performed numerically. This is a very difficult task, from a numerical analysis point of view, as we have to minimize the action on the space of vorticity paths (fields depending on a three dimensional space: two spatial dimensions plus time). This work can still be performed, as was done in a work in collaboration with J. Laurie. For instance figure 15 shows the most probable paths for the transition between parallel flows and dipoles (please see also figure 4, on page 6, for the observed transitions in the direct numerical simulations).

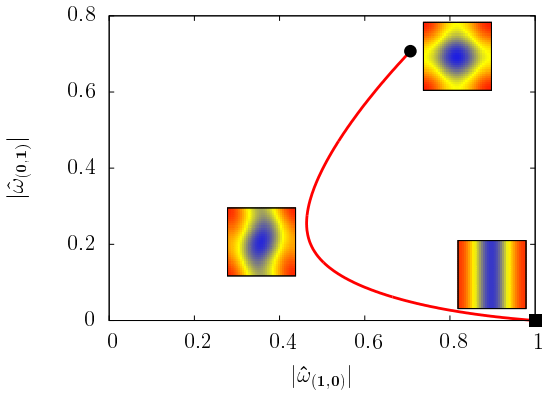

Fig. 15 Minimum action path between dipoles and parallel flows for the two-dimensional stochastic Navier-Stokes equations. For this example of noise correlation function C, the minimum action path involves mainly the two large scale modes. The path is represented in the the plane $\left(\left|\hat{\omega}_{(0,1)}\right|,\left|\hat{\omega}_{(1,0)}\right|\right)$, where $\hat{\omega}_{(0,1)}$ and $\hat{\omega}_{(1,0)}$ are the Fourier components of the vorticity field for the largest scales (**k**=(0,1) and **k**=(1,0)). The inset show how the vorticity field changes along the most probable path for the transition between zonal flows and dipole (please see also figure 4, on page 6, for the observed transitions in the direct numerical simulations).

Large deviations, the Freidlin–Wentzell formalism, and the WKB asymptotics

The discussion on section 4 is based on the computation of the transitions probabilities through path integrals (see Eq. (47), on page 22, Eq. (47) on page 30, and Eq.

(89), for the transition probabilities for the Kramer problem, the Quasi-Geostrophic Langevin dynamics and the Navier–Stokes equations respectively). As it is the case in quantum mechanics, such path integrals can be evaluated in two main cases: Gaussian cases, and in a semi-classical limit. In a semi-classical limit, when a parameter is small ($\hbar$ in quantum mechanics, $\Delta V/k_BT$ for the Kramer problem 47, γ for the Quasi-Geostrophic Langevin dynamics 47), the path integral can be evaluated as a Laplace integral. Then the path integral is equal to the exponential of the action of the most probable path (the least action path, or the classical path) multiplied by a prefactor that can be evaluated by considering Gaussian fluctuations around this most probable path (WKB or semi-classical asymptotic expansion). For instance for the Kramer problem, the result is

$$P(x_1,T;x_{-1},0) \underset{\sim}{^{1\ll T\ll \tau\exp(\beta\Delta V)}} \text{ and } {}^{\beta\Delta V\gg 1} \frac{T}{\tau}\exp\left(-\beta\Delta V\right), \tag{90}$$

as explained in section 24. Sometimes the following result is stated: for any time T

$$\lim_{\beta\to\infty}\frac{1}{\beta}\log P(x_1,T;x_{-1},0) = -\Delta V. \tag{91}$$

Such a result, using the logarithm of the transition probability and multiplying by the rate $1/\beta$, is called a large deviation result with rate $1/\beta$. This result is clearly weaker than the result 50, and also simpler to obtain as it involves only the least action path.

A question is to know under which conditions results like (90), or the large deviation result (91) are actually valid. This is a crucial question, as then the least action path gives the scaling of the transition probability and we can also conclude that most fluctuation paths concentrate close to the most probable one, the least action path. For any dynamical system of the type

$$\frac{\mathrm{dx}}{\mathrm{d}t} = F(x) + \sqrt{\varepsilon}\sigma(x)\eta,$$

where x is a vector of finite dimension n, η a white noise, $\sigma^T\sigma$ is a definite positive diffusion matrix, and the vector field F is such that the deterministic dynamics $\dot{x} = F(x)$ has isolated attractors, it is known that a large deviation result holds. In the mathematical literature, this is one of the subjects of Freidlin–Wentzell theory [30]. A more precise theorem can be found in classical literature [30, 67]. This theory corresponds to finite dimensional dynamics, with a clear small parameter (here the noise amplitude ε) and a clear separation of time scales (the system relaxes towards attractors on a time scale of order one, then getting deviations of order one needs very rare realizations of the noise). Clearly the Kramer problem discussed in section 4.1 fits into this Freidlin–Wentzell framework, with $\varepsilon = \beta\Delta V$.

A very subtle and interesting question is wether large deviation results hold for the Quasi-Geostrophic Langevin dynamics, discussed in section 4.2, in the limit $\gamma\to 0$. From the action, (47) on page 30, one clearly sees that a natural semi-classical small parameter, γ, does exist. Moreover, the deterministic dynamics actually re-

laxes on finite time towards the attractors which are the local minima of $\mathscr{G}$, as in the Freidlin–Wentzell framework. However the fact that the system describe the dynamics of a field, in infinite dimension, makes the result non-trivial. We do not discuss those subtle points further here.

For us, the most important issue is to understand if a large deviation result holds for the stochastic Navier–Stokes equations. Looking at the transition probability (89) and the Lagrangian 87, we see that no clear semi-classical parameter appears. One may wonder if the small noise amplitude α may be used as a semi-classical parameter. This is not clear at all. Indeed α is also the parameter that governs dissipation. For small α, on time scales of order 1, the dynamics is governed by the 2D Euler equation and the deterministic dynamics relaxes towards attractors of the 2D Euler dynamics, for instance towards equilibrium states described in section 3. However there are an infinite number of such equilibrium states, as they are parametrized by the energy and the vorticity distribution. Moreover those equilibrium states are not isolated, by contrast they form a connected set. Then we are clearly not within the hypothesis of Freidlin–Wentzell theory. Actually, the phenomenology, observed from experiments and numerical simulations (see figure 4, or [23, 10]), is that the dynamics is attracted by attractors of the two-dimensional Euler equations and then slowly drifts inside this set, on time scales that probably scale like $1/\alpha$ for small α.

The nature of the large deviations for such a systems with a connected set of attractors and a slow drift on a longer time scale might be not simple. A very interesting simple example, with only two degrees of freedom, is studied in [12]. In this paper, it is shown that a non standard large deviation rate may appear due to the possible slow drift along the set of attractors until the set of unstable fixed points of the deterministic dynamics.

A simpler phenomenology would be that large deviation occurs for transitions probabilities on time scale of order $1/\alpha$. This is for instance what actually happens in the Kramer problem in the underdamped limit as described in many classical references [32, 30]. Then a clear understanding emerges through first using the time scale separation in order to obtain a slow stochastic dynamics through stochastic averaging, and then obtain a large deviation result from this slow dynamics. We think that this is the most promising way towards understanding large deviations for the two-dimensional stochastic Navier–Stokes equations, and this is what we will discuss in section 5.

Before discussing stochastic averaging, let us first comment on simple empirical (numerical) facts about large deviations for the two-dimensional Navier–Stokes equations. Looking at the figure 4, and the discussion [10], we see that the transition between two different states is extremely rare: there is a clear time scale separation, as the typical transition time is 10^4 or 10^5 turn-over times. The simulations in the work [23] also show that the flow remains close to a well characterized attractor with weak fluctuations around it. These are clear signs of a large deviation regime. More precisely we can say from these empirical results that the invariant measure concentrates close to a set of states, that are stable steady states of the 2D Euler equations.

What is then the large deviation rate ? Following the stochastic averaging results presented in section 5, we will conclude that the slow dynamics is a deterministic dynamics plus a noise. The amplitude of the noise is related to the number of effective degrees of freedom in the fluctuations field close to the attractors (more precisely, the transverse degrees of freedom with respect to the attractor). Then we can conclude that the more we will force on the small scales, for a fixed total energy input rate, the smallest will be the noise in the slow dynamics, and the rarest will be large deviations. This can be also understood from a heuristic dynamical discussion: the process leading to the large scale structure and their fluctuations is a transfer of energy towards the largest scales, mainly through direct interaction with the large scale flow. Then if we exit more small scales modes with weaker amplitude, an averaging effect will tend to reduce fluctuations.

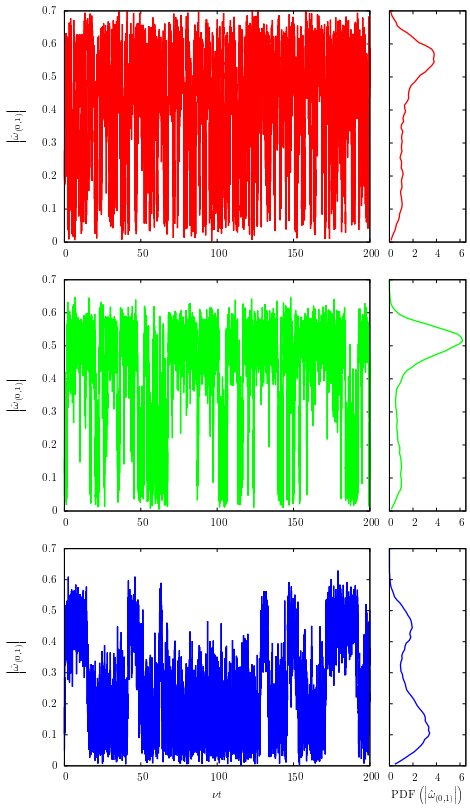

Fig. 16 Plot of the order parameter $\left|\omega_{(0,1)}\right|$ from direct numerical simulations of the two-dimensional Navier-Stokes equations, with aspect ratio $\delta = 1.09$, $\alpha = 0$ and $\nu = 7.10^{-4}$ (numerical simulations by E. Simonnet). The stochastic force spectrum is a flat spectrum forcing modes with Fourier coefficient with either $2 \leq k \leq 7$ (red, top), or $3 \leq k \leq 7$ (green, middle), or $4 \leq k \leq 7$ (blue, bottom). On the right-hand side of each time series is the PDF of $\left|\omega_{(0,1)}\right|$. This plot shows that the more Fourier coefficient are involved (the more we force on small scales), the rarest the transitions are. This is an indication that the typical scale of the forcing may be a large deviation rate.

An empirical evidence that the typical forcing scale may play the role of a large deviation rate is given on figure 16. This plot shows that the transition between dipole and parallel flow occurs less and less frequently as the stochastic force acts on smaller and smaller scales. The fact that the forcing scale (the number of effective degrees of freedom involved in the backward energy cascade) plays the role of a large deviation rate, does not mean that the time scale separation (small α and small ν) is not important. Actually it is likely that both the inverse of the time scale separation and typical scale of the stochastic force may be large deviation parameters. A better understanding requires further theoretical, numerical, and experimental works.

4.4.2 Non-equilibrium phase transitions in systems in rotating tank experiments

The study of non-equilibrium phase transitions has also been done in experiments in collaborations with M. Mathur and J. Sommeria. Experiments were performed in a water-filled 2m diameter annular tank at LEGI, Grenoble to simulate the interaction of mid-latitude atmospheric jets with continental topography. The tank rotates at a speed Ω_t to simulate the effects of earth's rotation. A linear bottom slope in the tank models the variation of the earth's background rotation with latitude. A jet was forced by an annular ring, rotating at a speed Ω_r with respect to the tank rotation, sitting on the surface of the water. The direct forcing mechanism allowed for an easy control of the zonal jet. On top of the linearly (in the radial direction) sloped tank bottom was a gaussian (in the azimuthal direction) shaped topography of amplitude 3cm to model continental topography. Velocity measurements in the two-dimensional plane 16cm below the free surface were performed using Particle Image Velocimetry.

Ω_t and Ω_r were the control parameters in our experiments. We define the order parameter C as the extent of propagation of the mode-3 wave in the azimuthal direction. Purely propagating and stationary mode-3 waves correspond to zero and a finite value, respectively, for the order parameter.

Figure 17(a) shows the variation of the order parameter C as a function of Ω_t from two experiments in which Ω_t is slowly increased (blue curve, experiment 1) and decreased (red curve, experiment 2) in time while Ω_r is held constant. For small values of Ω_t (0.45rad/s), C is small, indicating that the mode-3 wave is mostly propagating around the tank in both the experiments. For intermediate values of Ω_t, C attains very small values in experiment 1 and much larger values in experiment 2, showing that the system admits two different states (referred to as the propagating and blocked states, respectively) in the range $0.45 \leq \Omega_t \leq 0.53$rad/s. For larger values of Ω_t (0.55 rad/s), C settles at a finite (relatively large) value in both the experiments, indicating that the system attains the blocked state for large Ω_t irrespective of its history. The intermediate regime where both the propagating state and

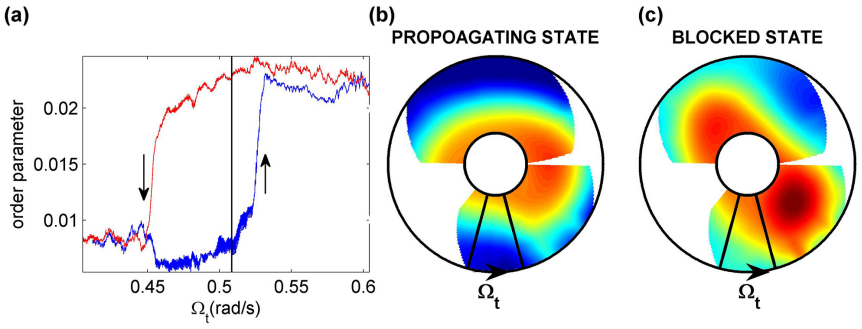

Fig. 17 (a) Order parameter C as a function of Ω_t in experiments where $\Omega_r = 0.78$rad/s is held constant. The two arrows indicate the direction in which Ω_t is varied in the corresponding experiments. The black vertical line corresponds to the value of Ω_r in the experiments presented in (b) & (c). (b) & (c) Time-averaged stream function ψ in experiments where $\Omega_t = 0.51$rad/s and $\Omega_r = 0.78$rad/s are both held constant. (b) & (c) correspond to the blue and red branches in (a), respectively.

the blocked state are possible for the same value of Ω_t is the region of bistability, a phenomenon admitted by systems exhibiting hysteresis.

Bistability is further demonstrated in figures 17(b) and 17(c), where we plot the time-averaged streamfunction as a function of the spatial coordinates from experiments in which $\Omega_r = 0.51$rad/s and $\Omega_t = 0.78$rad/s are both held constant. The propagating and blocked states are chosen by the path by which Ω_t is taken to $\Omega_t = 0.51$rad/s. The propagating state is characterized by a zonal-jet-like mean flow pattern whereas the blocked state is characterized by a cyclonic vortex downstream of the topography.

No spontaneous transitions between the propagating and the blocked state were observed, in spite of the strong turbulent fluctuations. Intrinsic noise in the form of cylindrical obstacles in the flow did not cause transitions either. External noise in the form of abrupt changes in Ω_t within the bistable regime causes switches between the two states. In the "mixed" state observed for relatively small values of Ω_t, the mode-3 phase variation with time shows step-like features and the computation of the statistics of the duration of each of step is currently ongoing. This work will be published soon.

4.4.3 Non-equilibrium phase transitions in systems with long-range interactions

In this section we briefly review two theoretical works [46, 47] which are directly related to the question of the bistability and of the existence of large deviations for the two-dimensional Navier–Stokes equations. The aim of these works was to find non-equilibrium phase transitions and bistability in systems described by the Vlasov equation with stochastic forces. The Vlasov equations have indeed mathe-

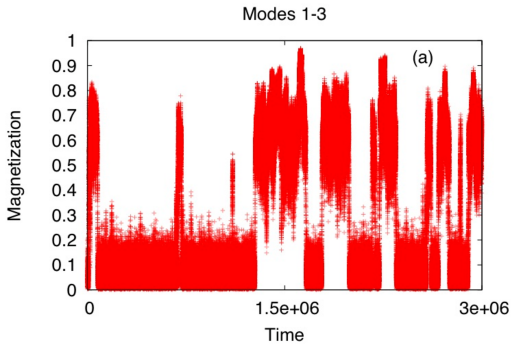

Fig. 18 Numerical simulation of non-equilibrium phase transitions for the stochastically-forced model with mean field interaction. The magnetization is plotted as a function of time at kinetic temperature T = 0.83. The figure shows clear signatures of bistability in which the system during the course of evolution switches back and forth between spatially homogeneous (magnetization of order 0) and inhomogeneous (magnetization of order 1) states.

matical and theoretical properties and behaviors which are very close to the two-dimensional Euler equations ones. Moreover, they are technically simpler to study, from a theoretical point of view, and a complete theoretical treatment could be done. This was the subject of two recent works [46, 47]. Under the effect of stochastic driving, the system at long times reaches stationary states where external forces balance dissipation on average. These states do not respect detailed balance, and are characterized by non-vanishing currents of conserved quantities. In order to analyze spatially homogeneous stationary states, we have developed a kinetic theory approach that generalizes the theory known for isolated long-range interacting systems. Our approach may also be generalized to describe spatially inhomogeneous stationary states. For homogeneous ones, we obtain a very good agreement between predictions from kinetic theory and extensive numerical simulations. In specific parameter regimes, our numerical simulation results show very interesting bistable behavior (non-equilibrium phase transition) between homogeneous and inhomogeneous states (please see figure 18). We advise any reader interested by the theoretical understanding of non-equilibrium phase transitions in turbulent flows to read the papers [46, 47].

5 Kinetic theory of zonal jet dynamics

As suggested in section 15, we will now use the fact that the large-scale flow evolves on a very long time scale (of order $1/\alpha$ for the stochastic barotropic equations (2) on page 9) in order to describe the large deviations that are observed over this long time scale (see figure 16). We present here this procedure, called stochastic averaging, in the case where the large-scale flow is constituted of zonal jets (parallel jets in the x direction).

The goal of the stochastic averaging is to obtain an effective equation that describes the slow dynamics of the large scales of the flow. Such a procedure, an example of turbulent closure, is usually inconsistent in a turbulence context. The main part of the work is thus to prove the consistency of the closure in this case. We do not describe this point in detail here, please see [15] for a complete presentation, but we present the main ideas in section 5.1. Assuming that the expansion is self-consistent, we will obtain the equation (100). The application of this equation in order to obtain a large-deviation result for the jets dynamics is then discussed in section 5.2.

5.1 Stochastic averaging

5.1.1 Rescaled dynamics

In the presence of a topography h or of a beta effect β, zonal jets are natural attractors of the inertial dynamics [15]. Then, in the presence of a small dissipation and of a small stochastic forcing (the regime $\alpha \ll 1$ in (2)), the flow will be very close to a zonal jet, plus a perturbation that corresponds to turbulent fluctuations, that vanish as α goes to zero. Moreover, as the zonal jet is a stationary solution of the inertial dynamics, it is expected to evolve over a time scale that is much larger than the time scale of evolution of the turbulence. In the units used in (2), the time scale of evolution of the turbulent fluctuations is of order one, while the time scale of evolution of the jet (the dissipation time scale) is $1/\alpha$. The goal of the stochastic averaging is to average the stochastic equations of motion over the realizations of this turbulent fluctuation field, in order to get the effective slow dynamics of the zonal jet.

The large scale zonal jets are characterized by either a zonal velocity field $\mathbf{v}_z(\mathbf{r}) = U(y)\mathbf{e}_x$ or its corresponding zonal potential vorticity $q_z(y) = -U'(y) + h(y)$. For reasons that will become clear in the following discussion (we will explain that this is a natural hypothesis and prove that it is self-consistent in the limit $\alpha \ll 1$), the non-zonal perturbation to this zonal velocity field is of order $\sqrt{\alpha}$. We then have the decomposition

$$q(\mathbf{r}) = q_z(y) + \sqrt{\alpha}\omega_m(\mathbf{r}) \quad , \quad \mathbf{v}(\mathbf{r}) = U(y)\mathbf{e}_x + \sqrt{\alpha}\mathbf{v}_m(\mathbf{r}) \tag{92}$$

where the zonal projection is defined by $\langle f \rangle (y) = \frac{1}{2\pi\delta}\int_0^{2\pi\delta} \mathrm{d}x\, f(\mathbf{r})$.

We now project the barotropic equation (2) into zonal and non-zonal part, assuming for simplicity that the random forcing doesn't act directly on the zonal degrees of freedom[1] ($\langle C \rangle = 0$):

$$\frac{\partial q_z}{\partial t} = -\alpha \frac{\partial}{\partial y}\left\langle v_m^{(y)}\omega_m \right\rangle - \alpha\omega_z + \nu\frac{\partial^2 \omega_z}{\partial y^2}, \tag{93}$$

[1] This assumption is not necessary for the theory, it is just for convenience.

$$\frac{\partial \omega_m}{\partial t} + L_U[\omega_m] = \sqrt{2}\eta - \sqrt{\alpha}\mathbf{v}_m.\nabla\omega_m + \sqrt{\alpha}\langle \mathbf{v}_m.\nabla\omega_m\rangle, \tag{94}$$

where L_U is the linearized dynamics operator around the zonal base flow U. We see that the zonal potential vorticity is coupled to the non-zonal one through the zonal average of the advection term $\frac{\partial}{\partial y}\left\langle v_m^{(y)}\omega_m\right\rangle$. If our rescaling of the equations is correct, we clearly see that the natural time scale for the evolution of the zonal flow is $1/\alpha$. By contrast, the natural time scale for the evolution of the non-zonal perturbation is one. These remarks show that in the limit $\alpha \ll 1$, we have a time scale separation between the slow zonal evolution and a rapid non-zonal evolution. Our aim is to use this remark in order to describe precisely the stochastic behavior of the Reynolds stress in this limit (by integrating out the non-zonal turbulence), and to prove that our rescaling of the equations and this time scale separation hypothesis is a self-consistent hypothesis.

5.1.2 Adiabatic elimination of fast variables

We will use the remarks that we have a time scale separation between zonal and non-zonal degrees of freedom in order to average out the effect of the meridional turbulence. This amounts at treating the non-zonal degrees of freedom adiabatically. This kind of problems are described in the theoretical physics literature as adiabatic elimination of fast variables [31] or may also be called stochastic averaging in the mathematics literature. Our aim is to perform the stochastic averaging of the barotropic flow equation and to find the equation that describes the slow evolution of zonal flows. In this stochastic problem, it is natural to work at the level of the probability density function (PDF) of the flow, $P[q] = P[q_z, \omega_m]$. Then, the dynamical equations (2) or (93,94) are equivalent to the so-called Fokker-Planck equation for P.

Complete Fokker-Planck equation

The evolution equation for the PDF reads

$$\frac{\partial P}{\partial t} = \mathscr{L}_0 P + \sqrt{\alpha}\mathscr{L}_n P + \alpha\mathscr{L}_z P, \tag{95}$$

The operator $\mathscr{L}_0$ is the Fokker-Planck operator that corresponds to the linearized dynamics close to the zonal flow U, forced by a Gaussian noise, white in time and with spatial correlations C. This Fokker-Planck operator acts on the non-zonal variables only and depends parametrically on U. This is in accordance with the fact that on time scales of order 1, the zonal flow does not evolve and only the non-zonal degrees of freedom evolve significantly. It should also be remarked that this term contains dissipation terms of order α and ν. These dissipation terms can be included in $\mathscr{L}_0$

because in the limit $\nu \ll \alpha \ll 1$, the non-zonal dynamics is dominated by the interaction with the mean flow, thanks to the so-called Orr mechanism. This crucial point will be discussed in the following paragraph. At order $\sqrt{\alpha}$, the nonlinear part of the perturbation $\mathscr{L}_n$ describes the non-linear interactions between non-zonal degrees of freedom. At order α, the zonal part of the perturbation $\mathscr{L}_z$ contains the terms that describe the large-scale friction and the coupling between the zonal and non-zonal flow.

Stationary distribution of the fast variables

The goal of our approach is to get an equation that describes only the zonal, slowly evolving part of the PDF, but taking into account the fact that the non-zonal degrees of freedom have rapidly relaxed to their stationary distribution. The first step is then to determine this stationary distribution of the non-zonal, fast evolving degrees of freedom. This stationary distribution is given by the stationary state of (95), retaining only the first order term: $\mathscr{L}_0 P = 0$. For the special case of a determined zonal flow $P[q_z, \omega_m] = \delta(q_z - q_0)\, Q(\omega_m)$, $\mathscr{L}_0$ is the Fokker-Planck operator that corresponds to the dynamics of the non-zonal degrees of freedoms, for quasi-geostrophic equations linearized around the base flow with potential vorticity q_0 (equation (94) without the non-linear terms.) It is a linear stochastic process (Ornstein–Uhlenbeck process) with zero average value, so we know that its stationary distribution is a centered Gaussian, entirely determined by the variance of ω_m. The variance is the stationary value of the two-points correlation function of ω_m, $g(\mathbf{r}_1, \mathbf{r}_2, t) = \mathbf{E}[\omega_m(\mathbf{r}_1, t)\omega_m(\mathbf{r}_2, t)]$. The evolution of g is given by the so-called Lyapunov equation, which is obtained by applying the Ito formula to the stochastic equation for ω_m:

$$\frac{\partial \omega_m}{\partial t} + L_U[\omega_m] = \sqrt{2}\eta \quad \Rightarrow \quad \frac{\partial g}{\partial t} + \left(L_U^{(1)} + L_U^{(2)}\right) g = 2C. \tag{96}$$

($L_U^{(i)}$ means that the operator is applied to the i-th variable). We now understand that the asymptotic behavior of this equation is a crucial point for the whole theory. It can be proved [9] that g has a well-defined limit (in the distributional sense) for $t \to \infty$, even in the absence of any dissipation mechanism ($\alpha = \nu = 0$). This may seem paradoxical as we deal with a linearized dynamics with a stochastic force and no dissipation mechanism. This is due to the Orr mechanism [9] (the effect of the shear through a non-normal linearized dynamics), that acts as an effective dissipation. The fact that (96) has a finite limit when $\alpha \to 0$ is the precise justification of the scaling (92), and it is thus the central point of the theory.

The average of an observable $A[q_z, \omega_m]$ over the stationary gaussian distribution is still a function of q_z, and it is an average over the non-zonal degrees of freedom, taking into account the fact that they have relaxed to their stationary distribution. In the following, we denote this average

$$\mathbf{E}_U[A] = \int \mathscr{D}[\omega_m] A[q_z, \omega_m] G[q_z, \omega_m], \tag{97}$$

the subscript U recalling that this quantity depends on the zonal flow.

Effective zonal Fokker-Planck equation

The formal development of the stochastic reduction is not reported here, see [15] for details. We obtain the following Fokker-Planck equation for the slowly evolving part of the zonal jets PDF $R[q_z]$,

$$\frac{\partial R}{\partial \tau} = \int \mathrm{d}y_1 \frac{\delta}{\delta q_z(y_1)} \left\{ \left[\frac{\partial F[U]}{\partial y_1} + \omega_z(y_1) - \frac{\nu}{\alpha} \frac{\partial^2 \omega_z}{\partial y_1^2} \right] R[q_z] \right\} \tag{98}$$

$$+ \int \mathrm{d}y_1 \mathrm{d}y_2 \frac{\delta^2}{\delta q_z(y_1) \delta q_z(y_2)} \left(C_R(y_1, y_2)[q_z] R[q_z] \right), \tag{99}$$

which evolves over the time scale $\tau = \alpha t$, with the drift term

$$F[U] = \mathbf{E}_U \left[\left\langle v_m^{(y)} \omega_m \right\rangle \right](y_1) + \alpha F_1[U],$$

with F_1 a functional of q_z, and the diffusion coefficient $C_R(y_1, y_2)[q_z]$, that also depends on the zonal flow q_z.

This Fokker-Planck equation is equivalent to a non-linear stochastic partial differential equation for the potential vorticity q_z,

$$\frac{\partial q_z}{\partial \tau} = -\frac{\partial F}{\partial y}[U] - \omega_z(y_1) + \frac{\nu}{\alpha} \frac{\partial^2 \omega_z}{\partial y^2} + \zeta, \tag{100}$$

where ζ is white in time Gaussian noise with spatial correlation C_R. As C_R depends itself on the velocity field U, this is a non-linear noise. The main physical consequences of this equation are discussed in the following paragraphs.

5.2 Physical interpretation of the zonal Fokker-Planck equation

5.2.1 First order: quasi-linear dynamics

At first order in α, we obtain a deterministic evolution equation for q_z:

$$\frac{\partial q_z}{\partial t} = -\alpha \frac{\partial}{\partial y} \mathbf{E}_U \left[\left\langle v_m^{(y)} \omega_m \right\rangle \right] - \alpha \omega_z + \nu \Delta \omega_z, \tag{101}$$

where the forcing term $-\alpha \frac{\partial}{\partial y} \mathbf{E}_U \left[\left\langle v_m^{(y)} \omega_m \right\rangle \right]$ can be computed as a linear transform of the stationary solution of the Lyapunov equation (96).

To summarize, we found that at leading order in α, the zonal flow is forced by the average of the advection term due to the non-zonal fluctuations (Reynolds' stress), and that this quantity is computed from the *linearized* dynamics for the fluctuations. In other words, we could have applied the same stochastic reduction technique to the quasi-linear dynamics (equations (93) and (94) without non-linear terms), and we would have obtained at leading order the same deterministic equation (101). The system (101,96) is a quasi-Gaussian (or second-order) closure of the dynamics. Working directly at the level of the PDF, and using the tools of the stochastic reduction, we have been able to justify the closure of this problem. This quasi-Gaussian closure has been already studied in numerical works (SSST in [29] and CE2 in [43]), and is known to give very good results.

Using again the results about the Orr mechanism [9], some important facts about equation (101) can be proved. First, we can make sure that the Reynolds' stress is well-behaved, even in the inertial limit $\alpha, \nu \to 0$, so that the zonal flow equation (101) is always well-defined. We can also show that the energy in the meridional degrees of freedom is of order α. As a consequence, a vanishing amount of energy is dissipated in the fluctuations and almost all the energy injected by the stochastic forcing goes to the zonal degrees flow. Moreover, the dynamics defined by equations (101,96) are much more simpler to solve numerically that the full non-linear dynamics (2). The numerical results that illustrate the two properties mentioned above are reported in figure 19.

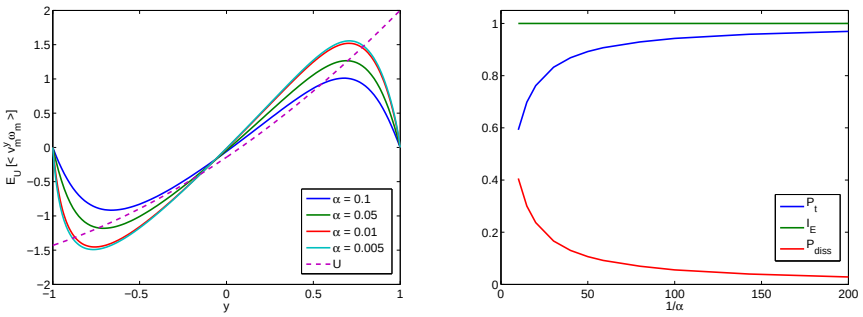

Fig. 19 Numerical results in the case of a parabolic base zonal flow $U(y) = A(y+2)^2 + U_0$ in a channel geometry, with a forcing at the scale $k_x = 1, k_y = 1$ and different values of the friction coefficient α, and $\nu = 0$. We see that in the inertial limit $\alpha \to 0$, the Reynolds' stress converges to a well-defined function, and that all the energy injected in the fluctuations is transferred to the zonal flow (blue line), while the energy dissipated in the fluctuations vanishes (red line). This constitutes a verification of the self-consistency of the theory, and relies on the non trivial Orr mechanism.

5.2.2 Next order: corrections and multistability and instantons

From the full Fokker-Planck equation (95), we expect the non-linear operator $\mathscr{L}_n$ to produce terms of order $\alpha^{1/2}$ and $\alpha^{3/2}$ in the zonal Fokker-Planck equation (99). The detailed computation shows that these terms exactly vanish. As a consequence, we have proved that the quasi-Gaussian closure (101,96) is correct in the limit $\alpha \ll 1$, with correction only at order α^2.

We then have a correction F_1 to the drift $F[U]$ due to the non-linear interactions. At this order, the quasilinear dynamics and non-linear dynamics differ. We also see the appearance of the noise term, which has a qualitatively different effect than the drift term. For instance if one is interested in large deviations from the most probable states, correction of order α to F_0 will still be vanishingly small, whereas the effect of the noise will be essential. This issue is important for the description of the bistability of zonal jets and phase transitions, as discussed in section 15.

6 Conclusion

During the last decade, there have been several advances in the statistical mechanics approach to two-dimensional and geostrophic turbulence. The most recent results, and possibly the most promising for geophysical application, is the use of large deviation theory in order to describe the attractors and the transition rates for the two-dimensional stochastic Navier-Stokes equations and geostrophic turbulence. We have described briefly some of those results in these lectures. Those encouraging results are still incomplete, and many open questions should be addressed by theoreticians in the future. Have those turbulent flow a large deviation regime ? What is the large deviation rate ? How to compute large deviation rate functions ? How to make those predictions effective in more complex models ? How to compute numerically large deviation rate functions for turbulent flows ?

This ongoing development of statistical mechanics approach to geophysical turbulent flows is extremely promising for many applications related to the turbulent part of climate dynamics. We expect very interesting outcomes in this direction in the future.

References

1. H. Aref. 150 Years of vortex dynamics. *Theoretical and Computational Fluid Dynamics*, 24:1–7, March 2010.
2. V. I. Arnold. An a priori estimate in the theory of hydrodynamic stability. *Izv. Vyss. Uchebn. Zaved. Matematika (1966) 3–5; Am. Math. Soc. Transl.*, 19:267–269, 1969.
3. M Berhanu, R Monchaux, S Fauve, N Mordant, F Pétrélis, A Chiffaudel, F Daviaud, B Dubrulle, L Marié, F Ravelet, M Bourgoin, Ph Odier, J.-F Pinton, and R Volk. Magnetic

field reversals in an experimental turbulent dynamo. *Europhysics Letters (EPL)*, 77(5):59001, March 2007.

4. Thierry Bodineau and Alice Guionnet. About the stationary states of vortex systems. In *Annales de l'Institut Henri Poincare (B) Probability and Statistics*, volume 35, pages 205–237. Elsevier, 1999.
5. C. Boucher, R. S. Ellis, and B. Turkington. Spatializing Random Measures: Doubly Indexed Processes and the Large Deviation Principle . *Annals Prob.*, 27:297–324, 1999.
6. F. Bouchet. Simpler variational problems for statistical equilibria of the 2d euler equation and other systems with long range interactions. *Physica D Nonlinear Phenomena*, 237:1976–1981, 2008.
7. F. Bouchet and J. Barré. Classification of Phase Transitions and Ensemble Inequivalence, in Systems with Long Range Interactions. *Journal of Statistical Physics*, 118:1073–1105, March 2005.
8. F. Bouchet and M. Corvellec. Invariant measures of the 2D Euler and Vlasov equations. *Journal of Statistical Mechanics: Theory and Experiment*, 8:P08021, August 2010.
9. F. Bouchet and H. Morita. Large time behavior and asymptotic stability of the 2D Euler and linearized Euler equations. *Physica D Nonlinear Phenomena*, 239:948–966, June 2010.
10. F. Bouchet and E. Simonnet. Random Changes of Flow Topology in Two-Dimensional and Geophysical Turbulence. *Physical Review Letters*, 102(9):094504, March 2009.
11. F. Bouchet and J. Sommeria. Emergence of intense jets and Jupiter's Great Red Spot as maximum-entropy structures. *Journal of Fluid Mechanics*, 464:165–207, August 2002.
12. F. Bouchet and H. Touchette. Non-classical large deviations for a noisy system with non-isolated attractors. *Journal of Statistical Mechanics: Theory and Experiment*, 5:28, May 2012.
13. F. Bouchet and A. Venaille. Statistical mechanics of two-dimensional and geophysical flows. *Physics Reports*, 515:227–295, 2012.
14. Freddy Bouchet and Jason Laurie. Statistical mechanics approaches to self organization of 2d flows: fifty years after, where does onsager's route lead to? *RIMS Kôkyûroku, Res. Inst. Math. Sci.*, 1798:42–58, 2012.
15. Freddy Bouchet, Cesare Nardini, and Tomás Tangarife. Kinetic theory of jet dynamics in the stochastic barotropic and 2d navier-stokes equations. *Journal of Statistical Physics*, 153(4):572–625, 2013.
16. Freddy Bouchet and Antoine Venaille. Statistical mechanics of two-dimensional and geophysical flows. *Physics Reports*, 515(5):227–295, 2012.
17. E. Brown and G. Ahlers. Rotations and cessations of the large-scale circulation in turbulent Rayleigh-Bénard convection. *Journal of Fluid Mechanics*, 568:351, November 2006.
18. E. Caglioti, P. L. Lions, C. Marchioro, and M. Pulvirenti. A special class of stationary flows for two-dimensional euler equations: A statistical mechanics description. Part II. *Commun. Math. Phys.*, 174:229–260, 1995.
19. B Caroli, C Caroli, and B Roulet. Diffusion in a bistable potential: The functional integral approach. *Journal of Statistical Physics*, 26(1):83–111, 1981.
20. M. Chandra and M. Verma. Dynamics and symmetries of flow reversals in turbulent convection. *Physical Review E*, 83(6):7–10, June 2011.
21. P. H. Chavanis. Statistical mechanis of two-dimensional vortices and stellar systems. In T. Dauxois, S. Ruffo, E. Arimondo, and M. Wilkens, editors, *Dynamics and Thermodynamics of Systems With Long Range Interactions*, volume 602 of *Lecture Notes in Physics*, pages 208–289. Springer-Verlag, 2002.
22. P. H. Chavanis and J. Sommeria. Classification of self-organized vortices in two-dimensional turbulence: the case of a bounded domain. *J. Fluid Mech.*, 314:267–297, 1996.
23. M. Chertkov, C. Connaughton, I. Kolokolov, and V. Lebedev. Dynamics of Energy Condensation in Two-Dimensional Turbulence. *Phys. Rev. Lett.*, 99:084501, 2007.
24. Marianne Corvellec and Freddy Bouchet. A complete theory of low-energy phase diagrams for two-dimensional turbulence steady states and equilibria. *arXiv preprint arXiv:1207.1966*, 2012.

25. T. E. Dowling and A. P. Ingersoll. Potential vorticity and layer thickness variations in the flow around Jupiter's Great Red SPOT and White Oval BC. *Journal of Atmospheric Sciences*, 45:1380–1396, 1988.
26. D. H. E. Dubin and T. M. O'Neil. Two-dimensional guiding-center transport of a pure electron plasma. *Phys. Rev. Lett.*, 60(13):1286–1289, 1988.
27. G. L. Eyink and H. Spohn. Negative-temperature states and large-scale, long-lived vortices in two-dimensional turbulence. *Journal of Statistical Physics*, 70:833–886, 1993.
28. G. L. Eyink and K. R. Sreenivasan. Onsager and the theory of hydrodynamic turbulence. *Rev. Mod. Phys.*, 78:87–135, 2006.
29. Brian F. Farrell and Petros J. Ioannou. Structural stability of turbulent jets. *Journal of Atmospheric Sciences*, 60:2101–2118, 2003.
30. M. I. Freidlin and A. D. Wentzell. *Random perturbations of dynamical systems*. Springer - New York, Berlin, 1984.
31. C. W. Gardiner. *Handbook of stochastic methods for physics, chemistry and the natural sciences*. Springer Series in Synergetics, Berlin: Springer, —c1994, 2nd ed. 1985. Corr. 3rd printing 1994, 1994.
32. P. Hänggi, P. Talkner, and M. Borkovec. Reaction-rate theory: fifty years after Kramers. *Reviews of Modern Physics*, 62:251–342, April 1990.
33. Corentin Herbert. Additional invariants and statistical equilibria for the 2d euler equations on a spherical domain. *Journal of Statistical Physics*, 152(6):1084–1114, 2013.
34. Corentin Herbert, Bérengère Dubrulle, Pierre-Henri Chavanis, and Didier Paillard. Statistical mechanics of quasi-geostrophic flows on a rotating sphere. *Journal of Statistical Mechanics: Theory and Experiment*, 2012(05):P05023, 2012.
35. Corentin Herbert, Raffaele Marino, and Annick Pouquet. Statistical equilibrium and inverse cascades of vortical modes for rotating and stratified flows. *Bulletin of the American Physical Society*, 58, 2013.
36. D. D. Holm, J. E. Marsden, and T. S. Ratiu. The Euler-Poincare Equations and Semidirect Products with Applications to Continuum Theories. In *eprint arXiv:chao-dyn/9801015*, page 1015, 1998.
37. G. Joyce and D. Montgomery. Negative temperature states for the two-dimensional guiding-centre plasma. *Journal of Plasma Physics*, 10:107, 1973.
38. M. K. H. Kiessling. Statistical mechanics of classical particles with logarithmic interactions. *Comm. Pure Appl. Math.*, 47:27–56, 1993.
39. M. K. H. Kiessling and J. L. Lebowitz. The Micro-Canonical Point Vortex Ensemble: Beyond Equivalence. *Lett. Math. Phys.*, 42(1):43–56, 1997.
40. Chjan C Lim, Xueru Ding, and Joseph Nebus. *Vortex dynamics, statistical mechanics, and planetary atmospheres*. World Scientific, 2009.
41. S. R. Maassen, H. J. H. Clercx, and G. J. F. Van Heijst. Self-organization of decaying quasi-two-dimensional turbulence in stratified fluid in rectangular containers. *Journal of Fluid Mechanics*, 495:19–33, November 2003.
42. A. J. Majda and X. Wang. *Nonlinear Dynamics and Statistical Theories for Basic Geophysical Flows*. Cambridge University Press, 2006.
43. J. B. Marston, E. Conover, and T. Schneider. Statistics of an Unstable Barotropic Jet from a Cumulant Expansion. *Journal of Atmospheric Sciences*, 65:1955, 2008.
44. J. Michel and R. Robert. Large deviations for young measures and statistical mechanics of infinite dimensional dynamical systems with conservation law. *Communications in Mathematical Physics*, 159:195–215, 1994.
45. J. Miller. Statistical mechanics of euler equations in two dimensions. *Phys. Rev. Lett.*, 65(17):2137–2140, 1990.
46. C. Nardini, S. Gupta, S. Ruffo, T. Dauxois, and F. Bouchet. Kinetic theory for non-equilibrium stationary states in long-range interacting systems. *Journal of Statistical Mechanics: Theory and Experiment*, 1:L01002, January 2012.
47. Cesare Nardini, Shamik Gupta, Stefano Ruffo, Thierry Dauxois, and Freddy Bouchet. Kinetic theory of nonequilibrium stochastic long-range systems: phase transition and bistability. *Journal of Statistical Mechanics: Theory and Experiment*, 2012(12):P12010, 2012.

48. A. Naso, P. H. Chavanis, and B. Dubrulle. Statistical mechanics of Fofonoff flows in an oceanic basin. *ArXiv e-prints:1007.0164*, 2009.
49. A. Naso, P. H. Chavanis, and B. Dubrulle. Statistical mechanics of two-dimensional Euler flows and minimum enstrophy states. *European Physical Journal B*, 77:187–212, September 2010.
50. J. J. Niemela, L. Skrbek, K. R. Sreenivasan, and R. J. Donnelly. The wind in confined thermal convection. *Journal of Fluid Mechanics*, 449:169, December 2001.
51. L. Onsager. Statistical hydrodynamics. *Nuovo Cimento*, 6 (No. 2 (Suppl.)):249–286, 1949.
52. L. Onsager and S. Machlup. Fluctuations and Irreversible Processes. *Phys. Rev.*, 91:1505–1512, 1953.
53. J. Pedlosky. *Geophysical fluid dynamics*. 1982.
54. Y Pomeau. Statistical approach (to 2D turbulence). In P. Tabeling and O. Cardoso, editors, *Turbulence: A Tentative Dictionary*, pages 117–123. Plenum Press, New York, 1995.
55. M. Potters, T. Vaillant, and F. Bouchet. Sampling microcanonical measures of the 2d euler equations through creutz's algorithm: a phase transition from disorder to order when energy is increased. *Accepted in, Journal of Statistical Mechanics: Theory and Experiment*, 2013.
56. Florent Ravelet, Louis Marié, Arnaud Chiffaudel, and Francois Daviaud. Multistability and memory effect in a highly turbulent flow: Experimental evidence for a global bifurcation. *Phys. Rev. Lett.*, 93(16):164501, 2004.
57. R. Robert. Etats d'équilibre statistique pour l'écoulement bidimensionnel d'un fluide parfait. *C. R. Acad. Sci.*, 1:311:575–578, 1990.
58. R. Robert. A maximum-entropy principle for two-dimensional perfect fluid dynamics. *J. Stat. Phys.*, 65:531–553, 1991.
59. R. Robert. On the Statistical Mechanics of 2D Euler Equation. *Communications in Mathematical Physics*, 212:245–256, 2000.
60. R. Robert and J. Sommeria. Statistical equilibrium states for two-dimensional flows. *J. Fluid Mech.*, 229:291–310, 1991.
61. R. Salmon. *Lectures on Geophysical Fluid Dynamics*. Oxford University Press, 1998.
62. M. J. Schmeits and H. A. Dijkstra. Bimodal behavior of the kuroshio and the gulf stream. *J. Phys. Oceanogr.*, 31:3435–56, 2001.
63. J. Sommeria. Experimental study of the two-dimensional inverse energy cascade in a square box. *Journal of Fluid Mechanics*, 170:139–68, 1986.
64. J. Sommeria. Two-Dimensional Turbulence. In Springer Berlin, editor, *New trends in turbulence*, volume 74 of *Les Houches*, pages 385–447, 2001.
65. K. Sugiyama, R. Ni, R. Stevens, T. Chan, S-Q. Zhou, H-D. Xi, C. Sun, K-Q. Grossmann, S.and Xia, and D. Lohse. Flow Reversals in Thermally Driven Turbulence. *Physical Review Letters*, 105(3):1–4, July 2010.
66. Simon Thalabard, Bérengère Dubrulle, and Freddy Bouchet. Statistical mechanics of the 3d axisymmetric euler equations in a taylor-couette geometry. *arXiv preprint arXiv:1306.1081*, 2013.
67. H. Touchette. The large deviation approach to statistical mechanics. *Physics Reports*, 478:1–69, 2009.
68. G. K. Vallis. *Atmospheric and Oceanic Fluid Dynamics*. 2006.
69. A. Venaille and F. Bouchet. Statistical Ensemble Inequivalence and Bicritical Points for Two-Dimensional Flows and Geophysical Flows. *Physical Review Letters*, 102(10):104501, March 2009.
70. A. Venaille, G. K. Vallis, and S. M. Griffies. The catalytic role of the beta effect in barotropization processes. *Journal of Fluid Mechanics*, 709:490–515, October 2012.
71. Antoine Venaille. Bottom-trapped currents as statistical equilibrium states above topographic anomalies. *arXiv preprint arXiv:1202.6155*, 2012.
72. E. R. Weeks, Y. Tian, J. S. Urbach, K. Ide, H. L. Swinney, and M. Ghil. Transitions Between Blocked and Zonal Flows in a Rotating Annulus. *Science*, 278:1598, 1997.
73. Peter B Weichman. Long-range correlations and coherent structures in magnetohydrodynamic equilibria. *Physical review letters*, 109(23):235002, 2012.
74. Jean Zinn-Justin et al. *Quantum field theory and critical phenomena*, volume 142. Clarendon Press Oxford, 2002.